GAMMA - GAMMA COINCIDENCE
and ANGULAR CORRELATION INVESTIGATIONS

A Thesis
Submitted to the
Faculty of Graduate Studies
University of Manitoba
in partial fulfillment of the
requirements for the degree of
Master of Science (Physics)

by

ANDREW JOHN DILAY

July, 1965

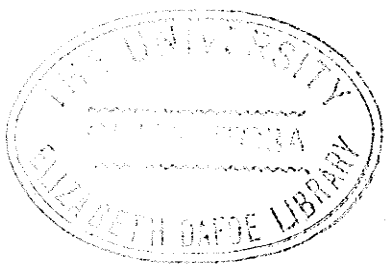

GAMMA - GAMMA COINCIDENCE

and

ANGULAR CORRELATION INVESTIGATIONS

- a thesis submitted to the Faculty of Graduate Studies, University of Manitoba, in partial fulfillment of the requirements for the degree of Master of Science (Physics) by Andrew John Dilay, July, 1965.

ABSTRACT

A gamma-gamma coincidence and 11-position angular correlation spectrometer capable of automatic operation is described and tested. In the decay of Se^{75}, gamma spectra in coincidence with the 122 kev and the weak 199 kev gamma rays have been investigated by a fast-slow coincidence technique (2τ = 70 nanoseconds). A gamma-gamma angular correlation run is performed on the 199-66 kev cascade and the value of $\frac{1}{2}$ for the spin of the 199 kev level in As^{75} is substantiated. Finally, some features of the high-energy (> 402 kev) region are described.

C O N T E N T S

LIST OF PLATES AND FIGURES

PREFACE

The work described herein was done at the University of Manitoba during 1964 and 1965.

The author wishes to express his heartfelt thanks and appreciation to Dr. S. I. H. Naqvi for his valuable advice, ideas, and his constant encouragement. The author is also indebted to Mr. W. R. Wall for his enlightening explanations on various topics in electronics, to Mr. R. S. Foulds for his aid in removing the "bugs" from the electronics, and to Drs. R. D. Connor, B. G. Hogg, and S. K. Sen for the loan of various scintillation detectors. Finally, the author would like to thank his fiancee, Miss Aloma Kadychuk, for her painstaking work and infinite patience in typing this thesis.

A research grant from the National Research Council of Canada supported the work and is gratefully acknowledged.

Chapter 1.

INTRODUCTION

A fundamental purpose of nuclear physics studies is the obtaining of information which will make it possible to understand the elemental basis of nuclear structure. Such an understanding is absolutely necessary if man desires to utilize fully the potentialities of the atomic nucleus, either as an energy source or as a means for providing knowledge that will contribute to the enrichment of human life.

A theoretical treatment of nuclear structure is considerably more complex than a corresponding treatment of atomic structure, primarily because the basic law of nuclear force still remains, to a great part, a mystery. With the advancement of the quantum theory came an essentially complete solution to the atomic problem since the only difficulties met lay in the application of quantum mechanics to systems governed entirely by the well known laws of electrodynamics. However, we have only the very barest phenomenological picture of the forces acting between nucleons. In fact, there is even doubt as to whether

we can justifiably regard the nucleons as elementary particles. Consequently, although there has been gathered an abundance of data and facts about nuclei, we have as yet been unsuccessful in our attempts to unite the facts into a consistent theory of the nucleus. We can merely describe various approaches to the problem, indicate the extent to which they have been successful, and also point out where they have broken down.

Historically, Becquerel's discovery of natural radioactivity in 1896, an indirect consequence of Roentgen's discovery of x-rays several months earlier, marked the birth of nuclear physics. Subsequent investigations divided the radiation into three distinct types now known as alpha, beta and gamma rays. In 1911 Ernest Rutherford laid the foundation of the modern theory of atomic structure with his classical paper in which he postulated that the atom consists not of a uniform sphere of positive charge (J. J. Thomson's plum-pudding model), but that all positive charge is concentrated in a relatively small region at the centre of the atom. This region was later called the nucleus of the atom. In 1919 Lord Rutherford broke up certain of these atomic nuclei and in 1934 Joliet and Curie showed that some of these artificial

nuclei were themselves radioactive, thus initiating an entirely new branch of research. Further studies have strongly pointed to the existence of energy levels within the nucleus itself, just as spectroscopic investigations showed the existence of atomic energy levels. This thesis will be concerned with a branch of nuclear spectroscopy, which is generally concerned with systematic arrangement and identification of the aforementioned nuclear energy levels.

In particular, we consider gamma ray spectroscopy. Gamma rays are electromagnetic radiation emitted from certain atomic nuclei due to some type of rearrangement within the nuclei leading to a lower energy content. Under the suppositions that there are a number of discrete energy levels within the nucleus and that ordinarily a nucleus is in the ground state, we consider the circumstances which must prevail in order for a nucleus to exist in an excited state. Experimentally, we find that alpha emitters exhibiting discrete alpha spectra are also gamma emitters, and similarly beta emitters are often gamma emitters. Subsequent energy measurements of the various radiations, together with the theory of beta decay, indicated that gamma emission is a result of a product nucleus being left in an excited state, i.e. a nucleus in its ground state cannot emit any gamma

radiation, so gamma decay occurs only as a consequence of those instances of alpha or beta emission, or electron capture, where the product nucleus is left in an excited state. A nucleus can also be excited in a scattering experiment, in which case it will emit gamma rays if the degree of excitation is insufficient for it to emit a particle. This implies that the last stages of most nuclear reactions involve gamma emissions.

Gamma ray spectroscopy provides a major source of knowledge of low-lying nuclear energy levels. This follows from the fact that gamma rays carry away angular momentum and explain changes in angular momentum, parity, and energy between the excited levels of a nucleus. Various specialized experimental techniques involve variations of what is referred to as the coincidence method, first introduced by Bothe and Geiger in 1925. One observes two or more ionizing events as detected by two or more respective detectors, which events have taken place within a predetermined time interval. In particular, we shall apply the coincidence method to gamma-gamma angular correlation studies wherein we shall record the coincidence counting rate of two successive gamma rays as a function of the angle between the propagation vectors of the gamma rays. Such a measurement enables one to calculate,

under favorable circumstances, the angular momenta of the relevant energy levels.

A pair of NaI(Tl) scintillation spectrometers served as the detectors in the coincidence and angular correlation work. The scintillation counter is discussed in the following chapter.

Chapter 2.

THE SCINTILLATION SPECTROMETER

Gamma ray spectroscopy is vitally dependent on accurate determinations of the gamma energies. However, one cannot, in general, use the same principles in gamma energy determinations as are used in energy determinations of charged particles. In the first place, gamma photons are uncharged, thus ruling out magnetic spectrometer methods. Secondly, the absorption of gamma rays by matter takes place not in a continuous fashion as does absorption of charged particles, but rather in a "yes - no" process in which aborption and scattering occur in single events. This implies that in observing a well collimated beam of gamma rays incident on some absorber, the collimated gamma rays which remain unattenuated have experienced virtually no absorption nor scattering, and conversely, any gamma rays which have experienced either absorption or scattering will be removed from the beam. i.e. There is either complete attenuation or none at all. Obviously this rules out energy determinations based on range measurements.

Techniques in gamma energy determinations must be based on interactions between gamma rays and matter and it

is found that the most significant of the possible interactions are the photo-electric effect, the Compton effect, and pair production. The definitions and discussions of these interactions can be found in many books on nuclear physics and in many theses (1), (2), (3), (4).

Since the end of World War II there have been many notable advancements in one of the earliest techniques of particle detection. This technique depends on the fact that certain materials scintillate on exposure to nuclear radiations. In particular, if a gamma ray is incident upon certain crystals, a rather complex process takes place, involving the initial formation of an excited electronic state of a small region of the crystal. This excess energy is promptly emitted as a very small flash of light, a scintillation.

Before the 1930's nuclear physicists had no efficient vacuum-tube circuits to simplify the counting of electrical pulses, and the scintillation method, involving wearisome visual counting and recording, was the sole method of alpha particle study. With the advent of vacuum-tube circuits and the Geiger-Müller tube, the scintillation method fell into disuse, but two developments in the mid-1940's hailed it back into popularity where it has remained ever since. First came the discovery of "phosphors" which not only scintillated on exposure to radiation, but which

were transparent to the light given off. This meant that one could use large volumes of these "phosphors" and thus enjoy an absorption efficiency far higher than ever before possible. A second obstacle to be overcome was the fact that a single scintillation is too feeble to be measured directly. The development of sensitive, efficient, high gain photomultiplier tubes (P. M. tubes) solved this problem.

Curran and Baker (5) in 1944 used a ZnS screen and an RCA 1P21 P. M. tube, connected to an oscilloscope, and detected 2 Mev alpha particles. Marshall and Coltman (6), (7), (8), in 1947-48 used a P. M. scintillation detector with a well-designed optical system to detect and count alpha particles, protons, fast electrons, gamma rays, x-rays, and neutrons. The main incentive to the scintillation method was provided in 1947 by H. Kallmann(9), who used a large clear crystal of naphthalene as a scintillator, and detected scintillations by beta and gamma rays with a P. M. tube. In 1948 Bell (10) found that crystalline anthracene is even better than naphthalene, giving pulses five times as great. It was then discovered (11) that there exists a class of scintillators, inorganic substances, which do not scintillate in the pure state but which scintillate strongly when "activated" with a certain substance. In particular Hofstadter (11) used thallium-activated sodium iodide crystals which produced pulses even

greater than anthracene, and the presence of the heavy element iodine made NaI(Tl) crystals especially useful for gamma ray detection. This follows because the high density NaI has a relatively high stopping power for gamma rays and has high photoelectric cross section and thus exhibits a high absorption efficiency. A 1950 report by McIntyre and Hofstadter (12) succeeded in establishing the NaI(Tl) scintillation spectrometer as an indispensible tool in gamma ray spectrometry.

Briefly describing the operation of a typical scintillation spectrometer, we have first the production of a scintillation described earlier (p. 7), followed by a photoelectric emission from the cathode of the P. M. as the feeble flash of light impinges on it, and finally the multiplication of the photoelectrons by secondary emission in successive stages until a measurable current is produced.

On examination of the output pulse from NaI(Tl), it is found that its size is very nearly in direct proportion to the energy of the incident gamma ray. It is interesting to look back and see how this question of linearity was finally settled. In 1950 Pringle and Standil (13) published a paper in which they reported, almost as an afterthought, a small degree of non-linearity in the scintillation response as a function of incident gamma energy, for $E_\gamma < 150$ kev. The nature

of the deviation was such that if E_γ is the abscissa, then the slope of the curve increased slightly and gradually from $E_\gamma \sim$ 150 kev to $E_\gamma \sim 0$. There arose an immediate storm of refutations from different research groups (14), (15), (16), (17), (18), who all claimed to have observed absolute linearity at least down to 1 kev, thus suggesting that the reported non-linearity (13) was due not to the crystal but rather to the accompanying electronics.

Since that time however, the result of Pringle and Standil has been confirmed by many researchers (19), (20), (21), and in fact the author has observed the effect, about which more will be said later.

Chapter 3.

THEORETICAL CONSIDERATIONS

3.1 Emission of Gamma Rays

Multipoles:

Details of this can be found in Segre (22). The electric and magnetic field vectors $\underline{E}$ and $\underline{H}$ can be shown (23) to be expressible as an expansion in terms of multipole components for outgoing waves. Performing this expansion yields two distinctly different types of terms, called electric and magnetic multipole components. Classically this corresponds to separating the radiation from some system of charges and currents into distinct types, depending on their angular distributions. Quantum mechanically, it corresponds to classifying the emitted gamma rays according to the amount of angular momentum $L\hbar$ they carry off. Several different angular momenta $L\hbar$ may be possible for a given gamma energy. L can take on only positive integral values, and L=0 is forbidden due to the transverse nature of electromagnetic waves. The component multipoles are specified by their order, 2^L, so that L=1 corresponds to a 2^1-pole, i.e. a dipole. Further, if the parity happens to be odd, then the radiation is referred to as E1 radiation, electric dipole radiation. If

the parity is even, then the radiation is denoted by M1, magnetic dipole radiation. In general, it is found that the parity change allowed equals the parity of the magnetic field, so E(L) transitions correspond with parity changes $(-1)^L$ and M(L) transitions correspond with parity changes $(-1)^{L+1}$. This rule regarding the parity changes is a consequence of the fact that the parity of the wave function of the entire system, which includes radiation as well as nucleus, must be conserved.

Selection Rules:

If $\underline{J}_i$ and $\underline{J}_f$ are total nuclear angular momentum vectors of initial and final states respectively, and if $\underline{L}$ is the angular momentum carried off by the gamma quantum, then conservation of angular momentum demands that

$$|J_i - J_f| \leq L \leq J_i + J_f \ .$$

The rules regarding the parities of the states can be written as

$$\pi_i \cdot \pi_f = (-1)^L \quad \text{for an E(L) pole,}$$

$$\text{and } \pi_i \cdot \pi_f = (-1)^{L+1} \quad \text{for an M(L) pole,}$$

where $\pi = +1$ corresponds to a state of even parity and $\pi = -1$ corresponds to a state of odd parity. Hence $\pi_i \cdot \pi_f = -1$ implies a parity change in the transition.

In considering transition probabilities, if it is assumed that the nuclear radius R is much smaller than the de Broglie wavelength $\lambda\!\!\!^{-}$ of the emitted gamma photon (i.e. $\frac{R}{\lambda\!\!\!^{-}} \ll 1$),

then it turns out that only the multipole components of lowest order will contribute appreciably. The assumption is good for most cases considered, so it is usually sufficient to consider only the lowest multipole order of each kind of radiation.

More explicitly, if $\pi_i \cdot \pi_f = (-1)^{J_i - J_f}$, then only $E(|J_i - J_f|)$ and $M(|J_i - J_f| + 1)$ radiation need be considered, whereas if $\pi_i \cdot \pi_f = (-1)^{J_i - J_f + 1}$, then only $M(|J_i - J_f|)$ and $E(|J_i - J_f| + 1)$ radiation are likely to be important. Furthermore, in the former case, where the electric component is of lower order than the magnetic component, the electric radiation generally eclipses the magnetic contribution. Such a transition is labelled a "parity-favored transition", while in a "parity-unfavored transition" the magnetic component is of lower order than the electric and the magnetic contribution is usually at least as important as is the electric.

3.2 Gamma-Gamma Angular Correlation

Gamma-Gamma Directional Correlations:

A considerably more general and exhaustive treatment of angular correlation of nuclear radiations is presented by Biedenharn and Rose (24), and in Siegbahn (25) and Segre (22). Only the basic principles involved and the major results required to interpret theoretically the particular angular cor-

relation work carried out by the author will be presented here.

The term "angular correlation" refers in general to both directional correlation and polarization correlation. The former allows determination of only (some of) the angular momenta of the pertinent nuclear energy levels and that of the emitted radiations, while the latter also enables one to determine the relative parities of the levels involved. This thesis will be concerned strictly with directional correlation. In ~~shall further restrict the investigations to direction-direction~~ double cascades only.

Consider a simple double cascade, as illustrated below, where the initial state has angular momentum J_α, the intermediate state J_β, and the final state J_γ. Also, let the first quantum carry off angular momentum L_ρ and the second quantum L_σ. Then, from the selection rules, it can be said

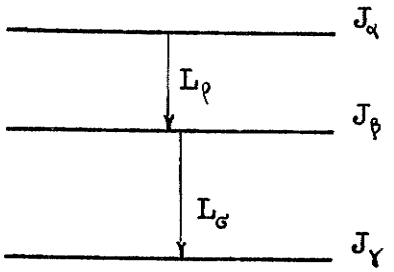

$$|J_\alpha - J_\beta| \leq L_\rho \leq J_\alpha + J_\beta$$

and $$|J_\beta - J_\gamma| \leq L_\sigma \leq J_\beta + J_\gamma .$$

Of special interest here is the relative probability $W(\theta)d\Omega$ that quantum σ enters a solid angle $d\Omega$ at an angle θ with respect to quantum ρ. Experimentally, it is the detectors which each subtend a solid angle $d\Omega$ at the centrally located source, and the detectors are at an angle θ one

from another. $W(\theta)$ is the correlation function. Ideally $W(\theta)$ represents the coincidence rate between quanta ρ and σ for the angle θ. However, the source is not a point and the solid angles are not infinitesimal, and thus the experimental coincidence rates are merely averages of $W(\theta)$ over angles θ varying about the angle between the axes of the two detectors. The necessary corrections will be mentioned later.

Following Segre (22), after considerable manipulation and simplification the result obtained for the theoretical correlation function is

$$W(\theta) = \sum_{n=0}^{n^{max}} A_{2n} P_{2n}(\cos\theta) \quad \text{with } A_0=1$$

$$= \text{const.} \sum_{n=0}^{n^{max}} B_{2n} \cos^{2n}\theta \quad \text{with } B_0=1$$

where P_{2n} is the Legendre polynomial

$$P_{2n}(\cos\theta) = \left(\frac{4}{4n+1}\right)^{\frac{1}{2}} Y_{2n,0}(\theta)$$

and n^{max} is the smallest of the numbers J_β, L_σ, L_ρ (if J_β is half integer, replace it by $J_\beta - \frac{1}{2}$). The coefficients are given by

$$A_{2n} = F_{2n}(L_\rho J_\alpha J_\beta) F_{2n}(L_\sigma J_\gamma J_\beta)$$

where F_{2n} are expressible by Clebsch-Gordan coefficients and Racah coefficients and are tabulated in Segre (22), pp. 380-383.

Geometrical Corrections:

The corrections employed to allow for the finite length of the source and for the finite solid angles subtended by the detectors are essentially those developed by Feingold and Frankel (26) in the section headed "Axial Source Corrections for Circular Detectors". For corrections due to the finite radius of the source the reader is referred to Manning and Bartholomew (27). They claim that to a first approximation the finite radius introduces a small negative $P_2(\cos\theta)$ term into the observed correlation function. Specifically, for a source one inch in diameter and four inches from the detector, the coefficient A_2 is replaced by $(A_2-0.02)$ for a distribution normalized to unity at 90^o. For a source one half inch in diameter and four inches from the detector, A_2 is replaced by $(A_2-0.005)$. In general it is found that the correction depends on the square of the radius of the source. The author used sources only 0.08 inches in radius, (i.e. about 0.16 inches in diameter) and a source-to-crystal distance of about four inches. The error involved was thus extremely small and in fact quite negligible as compared with the solid angle and finite length corrections.

The following is a brief outline of the finite source and solid angle corrections based on reference (26).

Later, in sec. 5.4, the corrections will be applied to a particular experiment.

Let ϵ_o be the length of the line source and let r_o be the distance from the centre of this axially placed source to the centre of the circular crystal face. Also, suppose the crystal has diameter "a".

The article (26) gives the true point-point correlation as

$$W(\theta') = \sum_l \frac{2l+1}{4\pi} a_l P_l(\cos\theta') \quad \ldots\ldots\ldots\ldots (1)$$

which, aside from a factor $\frac{4\pi}{a_o}$, is identical with the expression for the correlation given earlier in this section, where $A_2 = 5\frac{a_2}{a_o}$ and $A_4 = \frac{9a_4}{a_o}$. The experimental correlation is then given as

$$W(\theta) = \sum_l \frac{2l+1}{4\pi} h_l P_l(\cos\theta) \quad \ldots\ldots\ldots\ldots (2)$$

where $h_l = a_l b_l c_l = a_l b_l^2$, since $b_l = c_l$ for two identical detectors, the Legendre coefficients describing the efficiency functions of each detector. In terms of A_{2n}'s, equations (1) and (2) become respectively

$$W(\theta') = 1 + A_2 P_2(\cos\theta') + A_4 P_4(\cos\theta') \quad \ldots\ldots (3)$$

and

$$W(\theta) = 1 + \left(\frac{b_2}{b_o}\right)^2 A_2 P_2(\cos\theta) + \left(\frac{b_4}{b_o}\right)^2 A_4 P_4(\cos\theta) \quad \ldots\ldots (4).$$

To obtain the geometrical correction factors the article (26) gives

$$b_1 = \pi\alpha^2 \left\{ 1 + F_1\left(\alpha^2 + \frac{2}{3}\gamma^2\right) + F_2\left(\alpha^4 + \frac{3}{5}\gamma^4 + 2\alpha^2\gamma^2\right) \right\},$$

where $\alpha = \frac{a}{2r_o}$, $\gamma = \frac{\epsilon_o}{2r_o}$, and the coefficients F_1, F_2, as listed in table V of reference (26), are:

	F_1	F_2
b_o	-3/4	5/8
b_1	-1	1
b_2	-3/2	15/8
b_3	-9/4	7/2
b_4	-13/4	25/4
b_5	-9/2	85/8
b_6	-6	69/4

Chapter 4.

THE APPARATUS

4.1 General Description:

A schematic diagram of our spectrometer for gamma-gamma coincidence and angular correlation work is shown in fig. 1. A gamma ray entering one of the crystals results in a pulse emitted from the P.M. tube, which pulse then passes through a preamplifier (not shown). The preamplifier emits negative pulses, and since the pulse will eventually enter a gated biased amplifier (if certain conditions are satisfied) which accepts only positive pulses, it must be inverted. This is accomplished by the linear amplifier (L.A.) which also shapes it into a double delay line pulse (for coincidence purposes) and amplifies it according to the desired gain (see D.D.A. in fig. 1). The L.A. has two outputs, prompt and delayed, the latter being delayed by two microseconds. The prompt pulse must then satisfy predetermined upper and lower limits imposed by a fast speed discriminator and single channel analyzer (F.S.D. and S.C.A.) which each are patched into a fast/slow coincidence base unit. If a prompt pulse from the other F.S.D. and S.C.A. should happen to be in coincidence with the former prompt pulse, as well as satisfying

Fig. 1

Schematic Diagram of Gamma-Gamma Coincidence and Angular Correlation Spectrometer

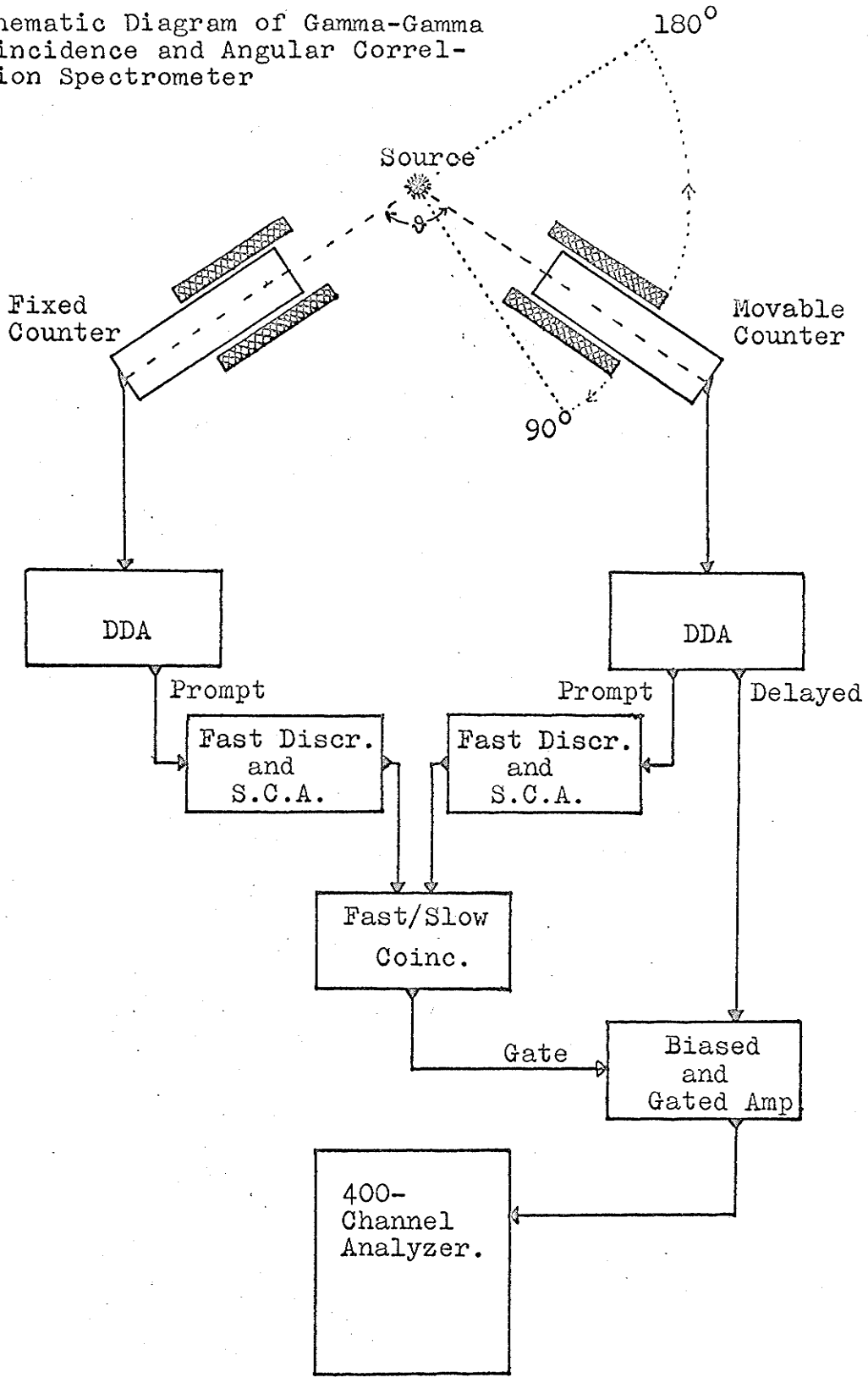

Plate 1.

Angular Correlation Spectrometer and Control Unit,
NaI(Tl) Detectors and Accompanying Electronics

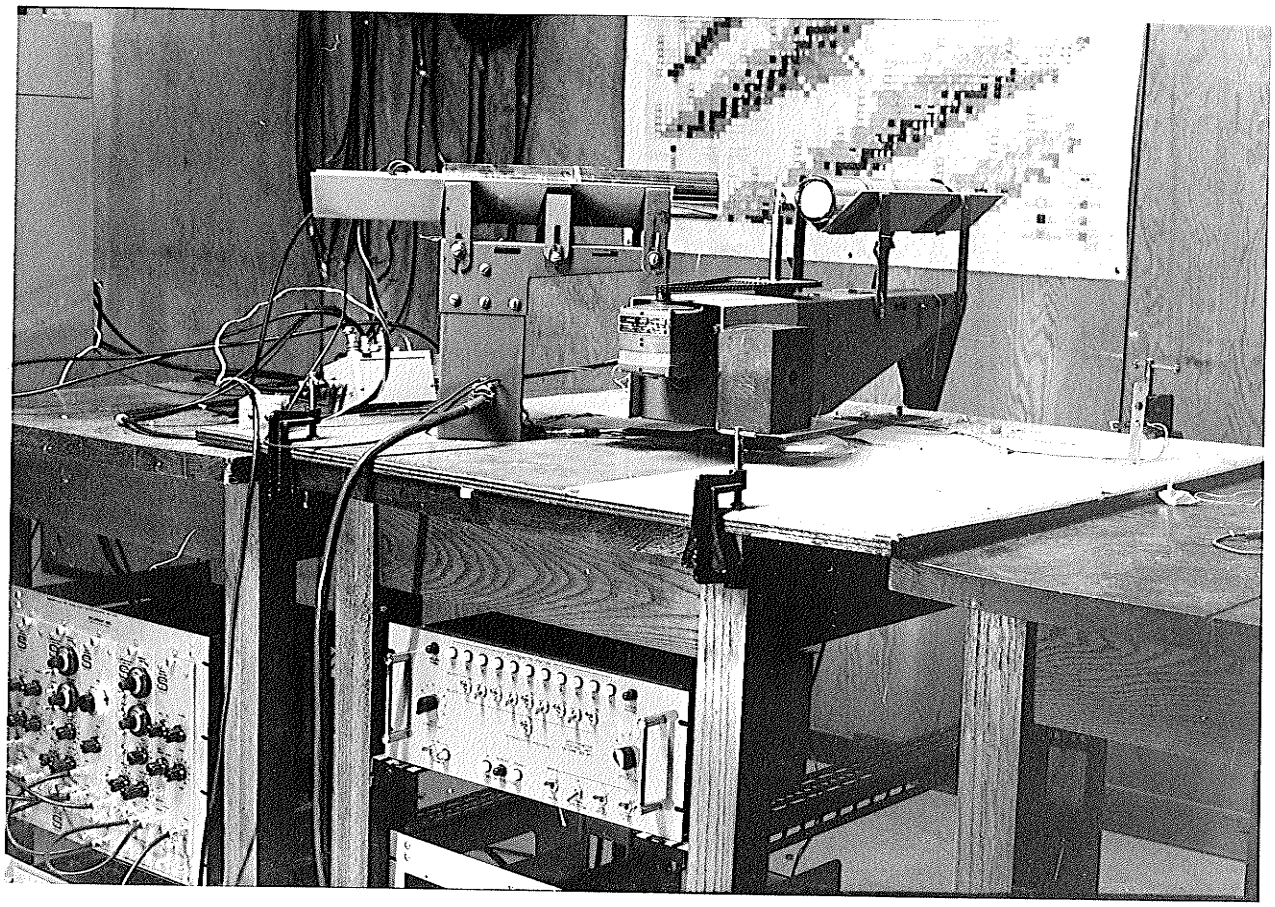

its own upper and lower limits, then the coincidence base unit generates a pulse which triggers the gate of the gated biased amplifier (B.A.), thus allowing the delayed pulse from the movable counter to enter the B.A. If this delayed pulse satisfies this final bias, it is allowed through to be analyzed in the four hundred channel Victoreen kicksorter.

Plate 1 shows the spectrometer table with its remote control unit, a source, the two NaI(Tl) detectors followed by their respective Victoreen preamplifiers, and the coincidence base unit containing the two L.A.'s, the two F.S.D. and S.C.A.'s, and the B.A.

4.2 Individual Descriptions

The Detectors:

Each of the two detector assemblies[1] consists of a 2"x2" NaI(Tl) crystal mounted on a 2" P.M. tube. Both detectors are differential type 88D76M, scintillation model 8A8N, P.M. tube Toshiba 7696. The detector of superior resolution (7.7% at 1100 volts) was used as the fixed detector, with which the window was set. The other detector (8% at 1000 volts) served as the movable detector. As shown in fig. 1, the pulses finally analyzed in the kicksorter were from

---

1 Kyoto Electronics Mfg. Co. Ltd., Kyoto, Japan
Purchased from Nuclear Enterprises Ltd., Winnipeg, Canada.

the movable detector. The detectors are such that one can remove the crystal by merely unscrewing the light-tight case, thus greatly simplifying any necessary repair work on the P.M. tube.

The preamplifiers were both Victoreen model 2277. A 400 channel Victoreen transistorized spectrometer, model ST400M, was used to analyze the pulses. The electronics[1] following the detectors and up to the kicksorter are patterned on the Yale system (28) where the L.A., F.S.D. and S.C.A., and F/S coincidence circuits are of Chase design (29), (30), and the B.A. is of Emmer design (31). The spectrometer control unit[2] was designed and built at Chalk River, Ontario.

Plate 2 shows the F/S coincidence base unit with the two L.A.'s, two F.S.D. and S.C.A.'s and the B.A. in the five available receptacles. Detailed descriptions, unit specifications, block diagrams, and circuit descriptions and diagrams can be found in the Sturrup Nuclear Instrumentation Manual. The following is intended to be only a very brief description of each unit.

---

1 Purchased from Sturrup, Incorporated, 50 Silver St., Middletown, Connecticut.

2 Purchased from Chalk River; 11-position spectrometer built by and purchased from Pritchard Engineering Co. Ltd., 70 Garry Street, Winnipeg.

Plate 2.

Fast-Slow Coincidence Spectrometer Control Panel

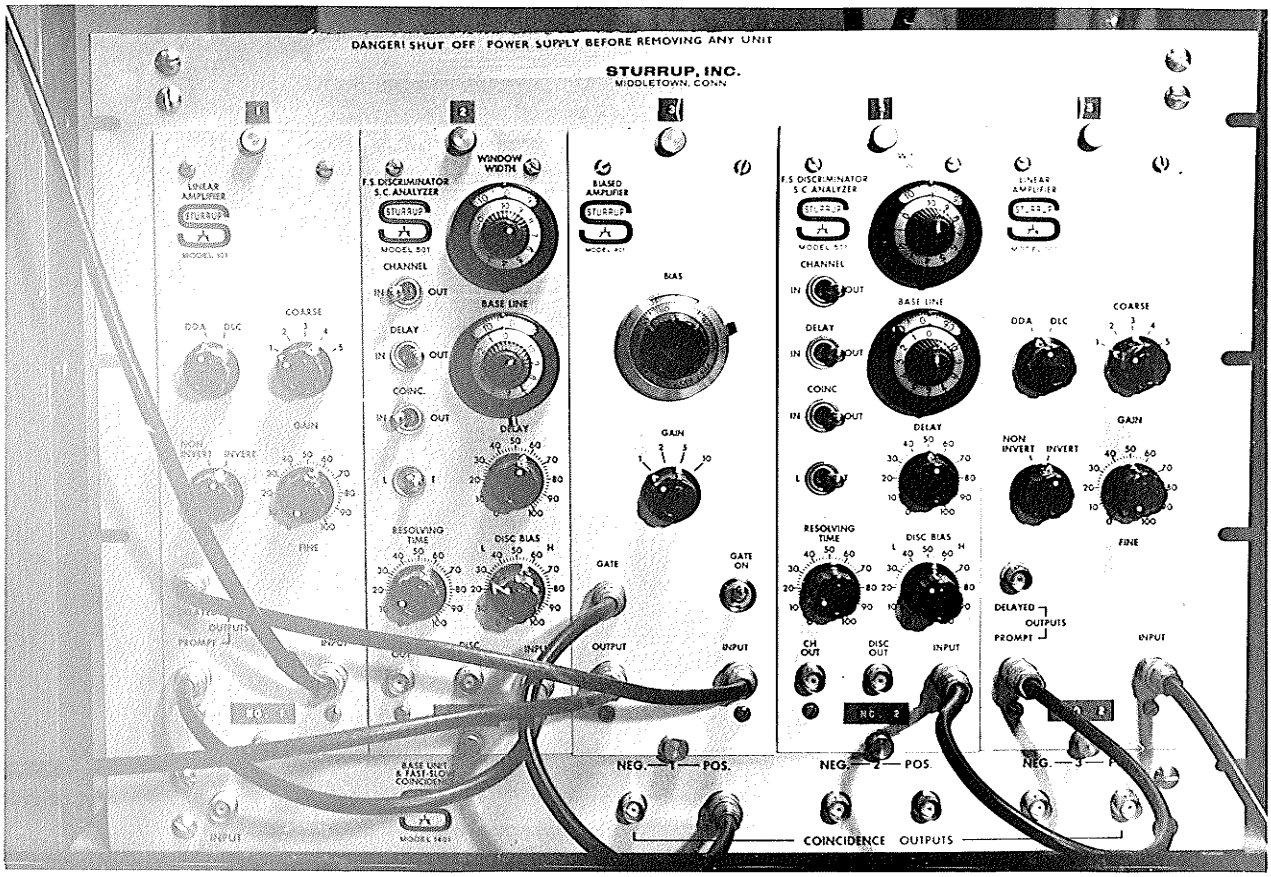

The Linear Amplifiers:

The linear double delay line amplifier model 101 (29) is a transistorized non-overloading amplifier. It can be switched into the symmetrical double delay line (D.D. L.) or single delay line clipped (D.L.C.) mode; has an approximate maximum gain of 600, with maximum pulse amplitude of ± 10 volts, and the capability of accepting up to 400 times overload without multiple counting. The prompt and 2 microsecond delayed outputs have been mentioned. Also there is switched pulse inversion, available as a front panel control.

The Fast Speed Discriminator and Single Channel Analyzer:

The model 501 F.S.D. and S.C.A. (30) has been designed for use with solid state or thermionic amplifiers over a wide range of input signals, which are switch selected for 0.5 to 10 volts and 5 to 100 volts.

The F.S.D. has two modes of operation, the leading edge of the pulse, and the crossover or trailing edge mode. Associated with this is a continuously variable coincidence resolving time of 10 to 180 nanoseconds. Coincidence times (2τ) can be set as low as 30 nanoseconds with little loss of genuine coincidence counts. A variable delay continuously adjustable over a 300 nanosecond range is used for compensating for differences in circuitry and detectors. Also one

can switch in a 400 nanosecond fixed delay for evaluating accidentals.

The S.C.A. selects the range of pulse amplitudes which generate the slow coincidence pulses, with the base line control setting the lower level and the window width setting the amplitude range above the base line. The duty cycle of the S.C.A. is controlled by a univibrator triggered from the F.S.D.

The Fast/Slow Coincidence Base Unit:

The model 1401 is a fully transistorized "fast/slow" coincidence base unit (30) with facilities for anti-coincidence and block inhibiting. The unit is designed not only as a fast/slow coincidence system but also as a five-receptacle base unit for a whole range of modules, including of course the L.A. model 101, the F.S.D. and S.C.A. model 501, and the gated B.A. model 401. i.e. These modules complement the fast/slow coincidence system.

There are three independent fast/slow coincidence circuits on each base unit, and each circuit can be patched to the fast and slow coincidence outputs of as many as five model 501 F.S.D. and S.C.A.'s. The outputs of each coincidence circuit are one positiveand one negative logic pulse, which pulses are generated only when all the model 501 F.S.D. and S.C.A.'s are in true coincidence.

The Biased Amplifier:

The model 401 gated B.A. (31) is the central unit in plate 2. It selects that portion of a positive input pulse above a selected bias level, for linear post amplification. The bias level is selected by a front panel control, through the range of 0.5 to 10 volts, and the post amplifier gain is step variable from 1 to 10. The amplifier gate is controlled so that only the required pulses are amplified, and all others are rejected. The input pulse may be positive single ended or bipolar. The output pulse is 10 volts positive maximum. It is linearly related to the incremental value of the input pulse above the bias level.

The Pulse Generator:

Not mentioned earlier since it was not used in actual data accumulation, the model 1501 pulse generator (Sturrup, Incorporated) was used for various test operations and calibrations. It is specifically designed to simulate a range of pulses from radiation detectors. This range runs from junction diodes to NaI(Tl) crystals and photomultipliers. It has a very short rise time with a long decay time which is necessary for the correct operation of the nuclear counting equipment.

Two outputs are provided, one of which is variable between 0 and 5.0 volts (unterminated) by the amplitude

control, and the second variable between 0 and 5.0 volts (terminated in 100 ohms) by means of the amplitude control and a step attenuator. The attenuator is used to set the maximum output voltage, and the amplitude control is used for differential continuous variations of output which are specified linear to better than 0.25%.

Pulse repetition rate is 60 p.p.s. The output is generated by a capacitor, charged to a specific voltage, being discharged across the output load by means of a mercury relay.

Rise time is step controlled with a front panel switch between 10 nanoseconds and 500 nanoseconds, with continuously variable fine control to increase the rise time by a factor of two.

The Angular Correlation Spectrometer:

For angular correlation work, one of the counters is fixed while the other can be moved such that it makes an angle θ between the limits of 90° and 180° with the fixed counter. The distance of both counters from the source is adjustable.

The spectrometer control unit is designed to provide manual or automatic control of the spectrometer from one to eleven counting positions. These positions are selected

by toggle switches on the front panel (see plate 1). Manual control of the spectrometer is provided for initial setting up procedure and may also be used to return the movable spectrometer arm to within its normal limits should a circuit failure cause it to go beyond these limits. Safety limit switches on the spectrometer itself provide automatic protection when the unit is operated in the automatic mode. Neons provide visual indication of the spectrometer's position and come in particularly handy if one is using a source strong enough to warrant considerable separation between the spectrometer table (where the source is) and the control unit (where the researcher is).

The movable counter can be programmed to stop automatically at any combination of numbers between and including one and eleven. This is accomplished by setting the correct combination of toggle switches and limit switches. A toggle switch on the back determines whether the counting is to be done only as θ increases, or only as θ decreases, or both. The movable counter stops at the first selected position, counts for the time interval specified by the kicksorter timer, and at the end of this time the control unit receives a -6 volt pulse from the kicksorter, which then begins the destructive readout operation while the movable counter advances to the next pre-

selected spectrometer position. When both the spectrometer advance action and the destructive readout operation are complete, the control unit provides a signal (momentary closure of contacts) to the kicksorter which resets and begins a new counting operation at the new position. This entire procedure is repeated at each position of the preselected combination. The readout operation was recorded with a Hewlett Packard Digital Recorder model 562A[1].

As can be seen from plate 1, the movable spectrometer arm was weighted at the short end with lead bricks to counteract the tilt produced in the arm by the weight of the detector. This was necessary to ensure that the movable arm swept out a single plane, an important requirement in angular correlation work.

The source holders were lucite cylinders, 0.64 cm. in diameter, and 5 cm. long, with a hole drilled down the centre, 0.4 cm. in diameter and 3 cm. long. In preparing the sources, the desirable strength of source was concentrated into as small a volume as deemed practical since this would obviously reduce correction factors for finite source size.

---

1 The author is indebted to Dr. K. I. K. Roulston for the use of this recorder.

Chapter 5.

PERFORMANCE TESTS

5.1 The Linear Amplifiers:

The pulse generator was inserted into the central receptacle, normally occupied by the biased amplifier, and pulses of 10 nanoseconds rise time were fed into each of the linear amplifiers. The prompt and delayed outputs of each amplifier were examined on a 515A Tektronix oscilloscope and after various circuit adjustments both amplifiers produced excellent double delay line pulses of rise time and width quite close to those specified in the Sturrup manual.

Assuming the pulse generator to be linear within its claim of 0.25%, it was then used to test the linearity of the amplifiers by feeding the prompt output of the amplifier into the Victoreen 400-channel kicksorter and plotting the channel with the maximum number of counts versus the pulse generator amplitude setting. A curve was obtained for various settings of the amplifier coarse and fine gain controls, and fig. 2 illustrates the result for L.A. #1. For each gain setting, the points form a virtually straight line, with deviations well within the specified 1% linearity. L.A. #2 yielded a similar result.

5.2 The Single Channel Analyzer:

The windows of the S.C.A.'s were checked using a

Fig. 2

Linearity of Linear Amplifier #1

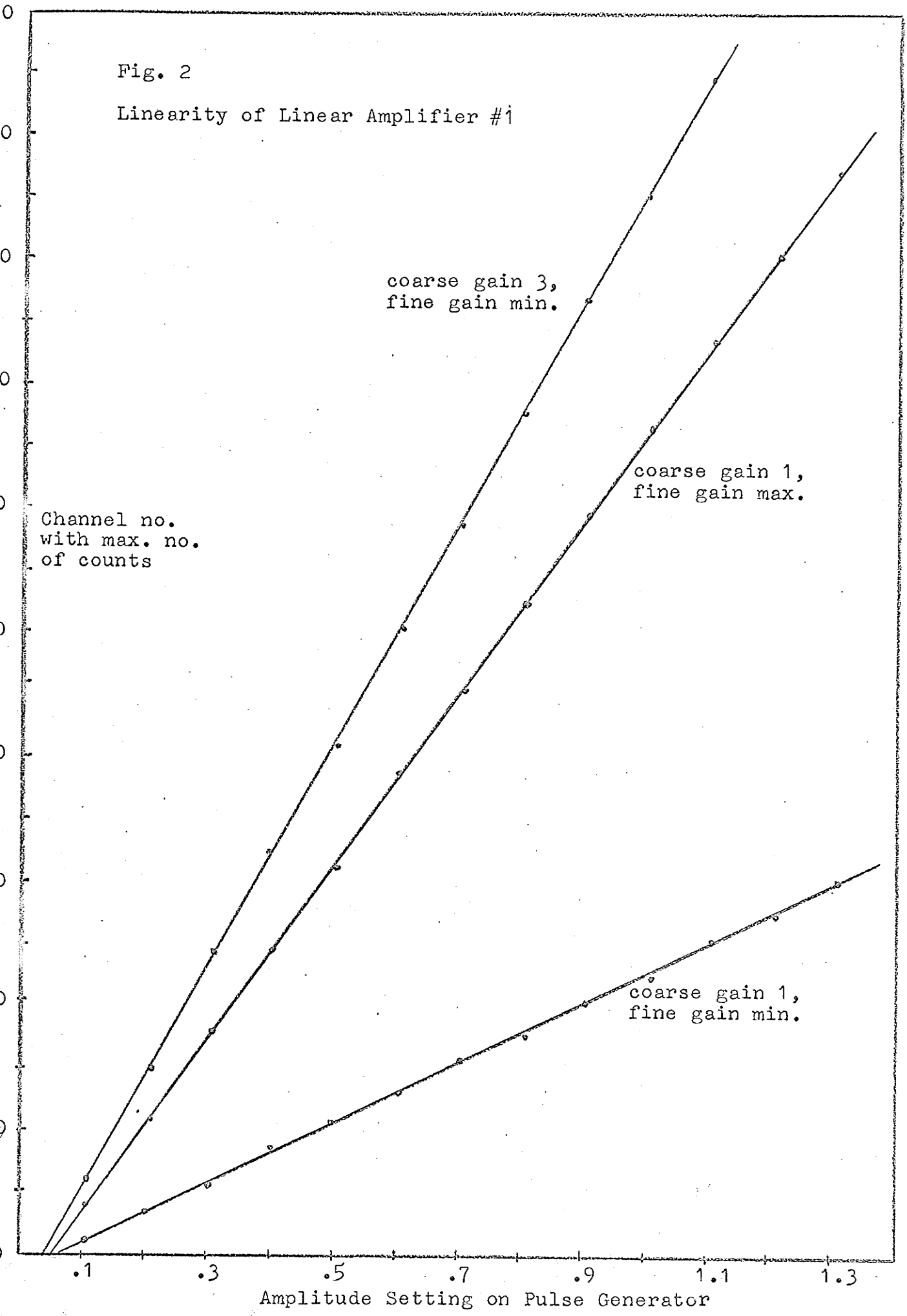

Fig. 3

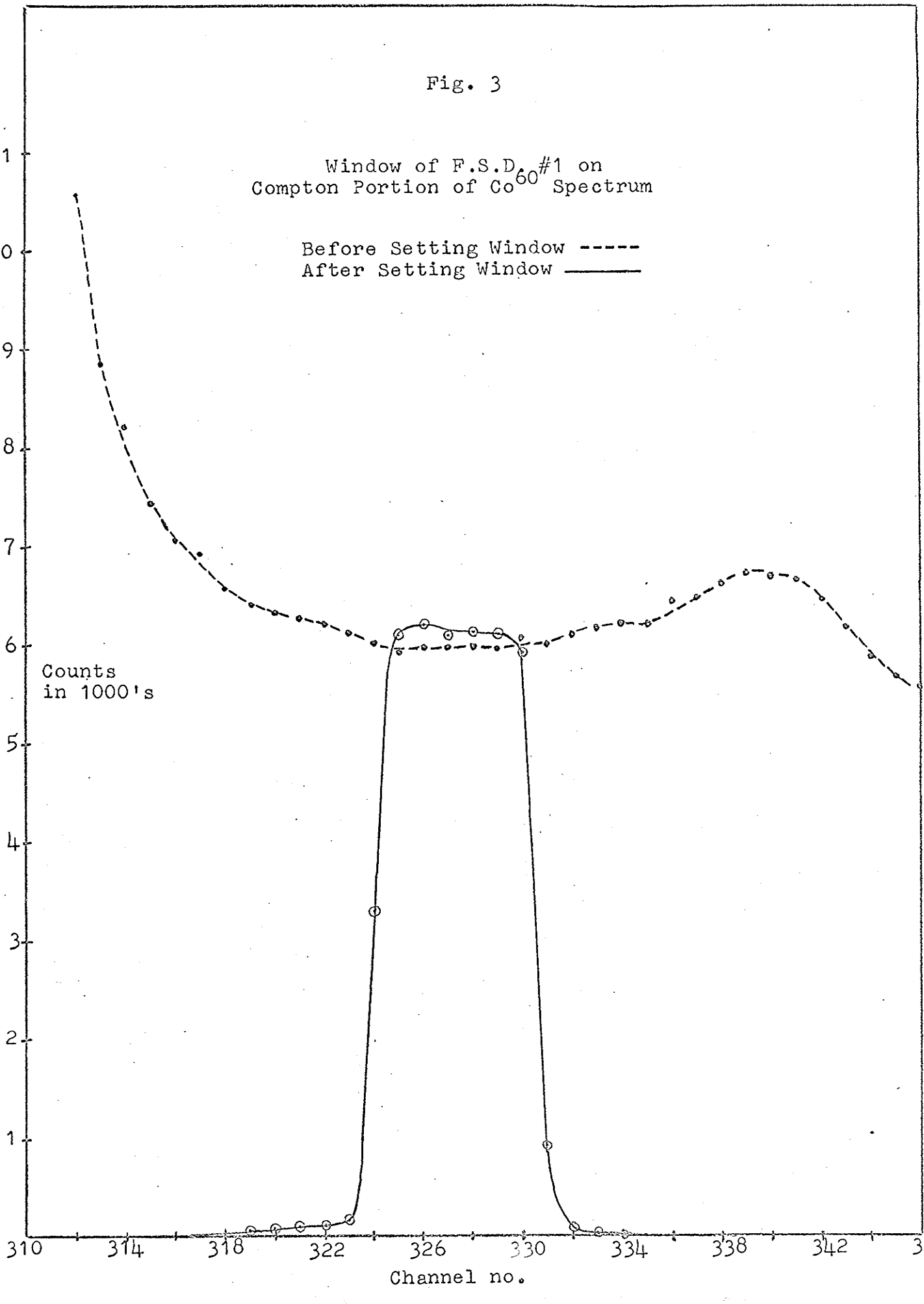
Window of F.S.D. #1 on
Compton Portion of Co60 Spectrum
Before Setting Window -----
After Setting Window ———
Counts
in 1000's
1
0
9
8
7
6
5
4
3
2
1
310
314
318
322
326
330
334
338
342
346
Channel no.

single detector, linear amplifier, biased amplifier, and kick-sorter. A complete singles spectrum of Co^{60} was obtained by setting a minimum base line and maximum window width of the S. C.A., and by leaving the B.A. bias at zero. Then, having printed out the spectrum, the window width was reduced to about 100 kev and the base line raised until the 100 kev window was situated in an appropriately flat part of the spectrum. This part turned out to be in the middle of the Compton portion. A spectrum of this window was then accumulated until the statistics were similar to that of the former spectrum. The two spectra were then compared to check qualitatively the degree of sharpness of the window. As is indicated in fig. 3, the window is quite "clean" in that the upper and lower cutoffs occur very sharply (i.e. from maximum height to essentially zero in about 38 kev). A similarly"clean" window was obtained from S.C.A. #2.

5.3 The Fast Speed Discriminator and Coincidence Base Unit:

Preliminary tests revealed a few dry joints and a diode in backwards in the S.C.A.'s. Also, the resolving time control of F.S.D. #1 was found to be disconnected. Having cleared up these minor difficulties, tests were then begun on the performance of the fast/slow coincidence process.

Of major importance in most coincidence work is the setting of a resolving time τ which is small enough to exclude

most accidental coincidences and large enough to avoid loss of genuine coincidences. The particular resolving time used generally depends on the cascade being investigated and for the cascades studied here, resolving times between 25 nanoseconds and 35 nanoseconds were found quite satisfactory. In the following will be described the technique used to obtain a rough setting of a desired resolving time. The accuracy of this rough setting will then be checked.

The object of the test was to set a resolving time of about 24 nanoseconds. Using a 20 microcurie Co^{60} source the prompt output pulse of each linear amplifier was observed on the 515A scope and the amplifier gains were set such that the maximum pulse from each amplifier was 9 volts. The pulse generator was then inserted into the middle receptacle and its pulses were fed simultaneously into the two linear amplifiers. The pulse amplitude was adjusted until the two linear amplifiers were each putting out 9 volt pulses, as observed on the scope. The fast speed discriminators were put into the crossover, or trailing edge coincidence mode and, together with the single channel analyzers, were patched into the fast/slow coincidence base unit.

Each of the 100 divisions on the continuous delay control of F.S.D. #1 was found to represent 3.2 nanoseconds delay, and for F.S.D. #2, each division represented 3.4 nanoseconds delay. In general, the full width at half maximum (F.W.H.M.)

of the eventual delay curve represents 2τ, which is about 48 nanoseconds in this case. This is about 15 divisions on F.S.D. #1. The positive coincidence output was fed into the 515A scope, and with the continuous delay of F.S.D. #2 fixed at 50, the resolving time panel controls of both F.S.D.'s were adjusted until a coincidence output appeared on the scope. The continuous delay of F.S.D. #1 was varied and note was taken of the highest delay and also of the lowest delay at which the coincidence output appeared. The resolving time controls were lowered (or raised) until the difference between these two delays was about 15 divisions (48 nanoseconds). This, it was hoped, was the desired resolving time setting. For this particular test, the desired delay difference of 48 nanoseconds occurred for a resolving time control setting of 12.5 for both F.S.D.'s.

To obtain a far more accurate measure of the resolving time, the coincidence counting rate was plotted as a function of the delay setting of F.S.D. #1, again using Co^{60} as the source. See fig. 4. Notice the maximum coincidence counting rate occurs for a delay setting of 51.5 and that the F.W.H.M. is about 53 nanoseconds, $=2\tau$. Thus $\tau = 26.5$ nanoseconds, within 3 nanoseconds of the predicted resolving time.

This is very good agreement and allows one to make reasonably accurate resolving time settings quickly, without having to plot an entire delay curve every time. After making rough

Fig. 4

Delay Curve of F.S.D. #1,
with Delay of F.S.D. #2 Fixed

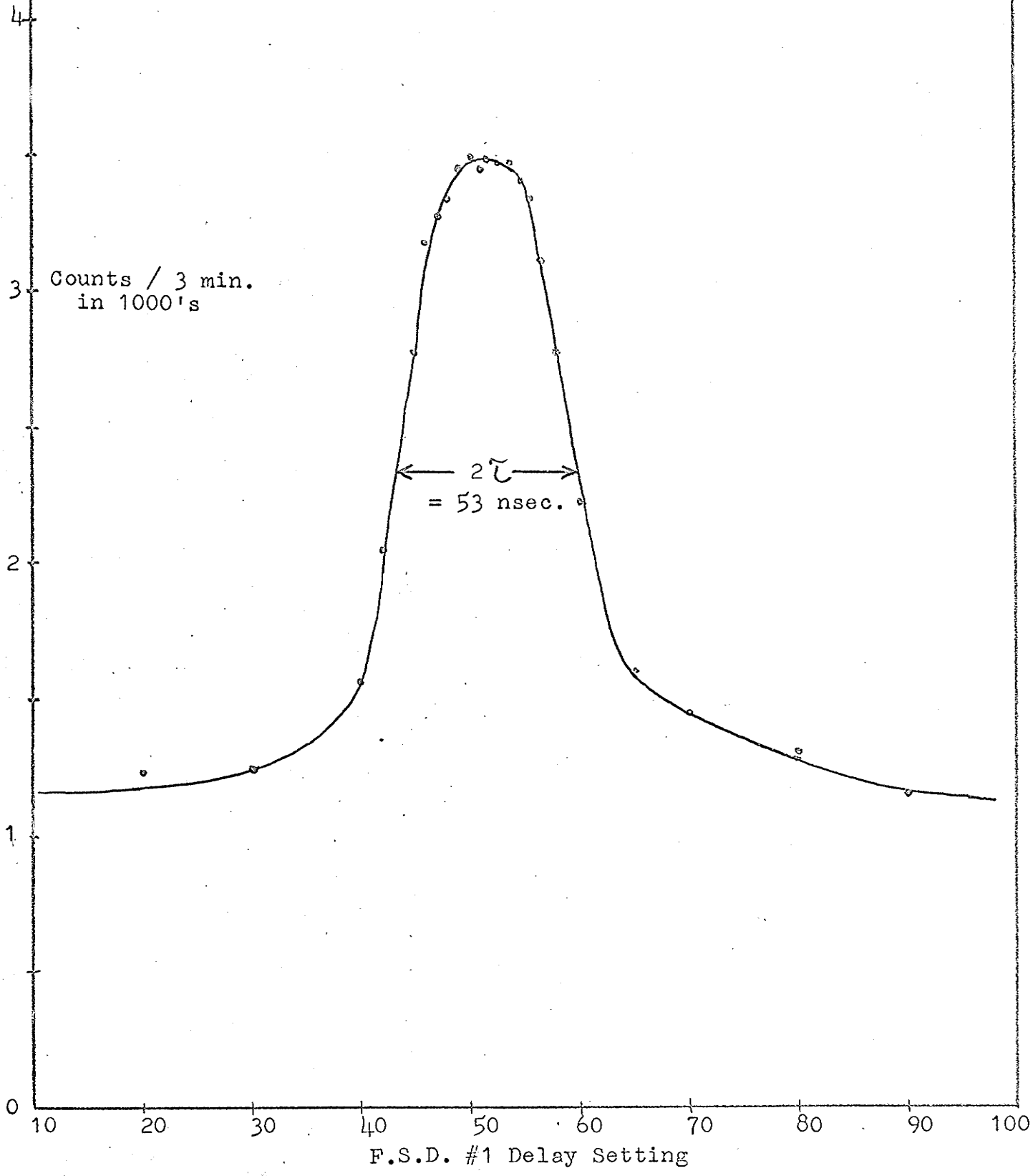

settings with the pulse generator, one need merely plot a few points of the delay curve (using the source) to determine the delay setting which gives the maximum coincidence counting rate.

5.4 Angular Correlation Spectrometer:

The angular correlation spectrometer was tested by checking the asymmetry for Co^{60}, and the isotropy which should be produced by Na^{22}.

Co^{60} Asymmetry

As the first test for the angular correlation spectrometer, the magnitude of the correlation for Co^{60} was determined both experimentally, and then checked theoretically, using the geometrical corrections (26). The magnitude is expressed by the asymmetry A, which may be defined as

$$A = \frac{W(180^{\circ})}{W(90^{\circ})} \quad \ldots\ldots\ldots\ldots\ldots\ldots \quad (1) \quad .$$

The decay scheme of Co^{60} is shown below.

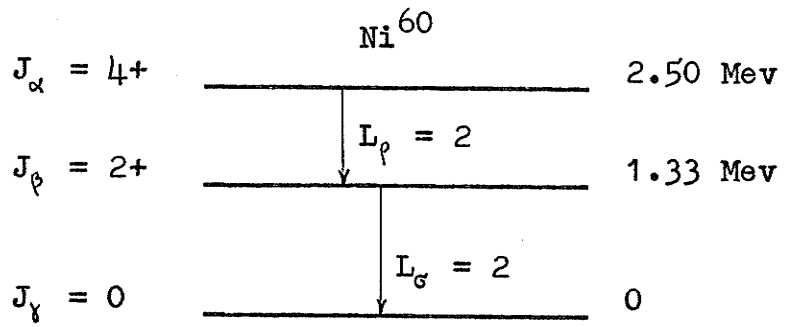

Co^{60} decays by beta rays mainly to the 4+ state in Ni^{60}, followed by the cascade 4(2)2(2)0 to the Ni^{60} ground state.

The correlation function defined in sec. 3.2 yields the well-established correlation for Co^{60}:-

$$W(\theta) = 1 + 0.1020\ P_2(\cos\theta) + 0.0091\ P_4(\cos\theta) \quad \ldots\ldots\ldots (2).$$

Then, since

$$P_2(\cos 90^\circ) = -0.5, \quad P_4(\cos 90^\circ) = 0.375,$$

$$P_2(\cos 180^\circ) = P_4(\cos 180^\circ) = 1,$$

the uncorrected theoretical asymmetry is

$$A = \frac{1 + 0.1020 + 0.0091}{1 - 0.0510 + 0.0034} = 1.167.$$

Now consider the geometrical corrections (26), outlined in sec. 3.2 of this thesis.

Experimentally, the Co^{60} source was of about 65 microcuries strength and was concentrated in a very small region of the source holder (one tiny drop about 1 mm. in diameter). Thus, $\epsilon_o = 0$ for all intents and purposes (i.e. $\gamma = 0$). Also, $r_o = 10.63$ cm. and $a = 4.445$ cm. Following through, the calculations yield $b_o = 0.13299$, $b_2 = 0.12882$, $b_4 = 0.11946$.

Thus $\left(\frac{b_2}{b_o}\right)^2 = 0.938$, and $\left(\frac{b_4}{b_o}\right)^2 = 0.807$. From equation (4) in sec. 3.2, the corrected correlation function is then

$$W(\theta) = 1 + 0.938\ A_2 P_2(\cos\theta) + 0.807\ A_4 P_4(\cos\theta),$$

where $A_2 = 0.1020$ and $A_4 = 0.0091$ for Co^{60}, as given in equation (2) of sec. 5.4. Then, from equation (1) of sec. 5.4, the corrected theoretical asymmetry is

$$A = \frac{1 + 0.938\ A_2 + 0.807\ A_4}{1 - (0.938)(A_2)(0.5) + (0.807)(A_4)(0.375)} = 1.155.$$

The experimental asymmetry was obtained by taking the ratio of the area under the 1.33 Mev-gated coincidence photopeak for $\theta = 180^\circ$, to the area for $\theta = 90^\circ$. Resolving time was about 24 nanoseconds. The coincidence photopeaks were each at 1.17 Mev of course (see Co^{60} decay scheme), and the areas taken (with a planimeter) were the areas of Gaussian curves[1] which had been fitted carefully to each photopeak. The formula used to fit the Gaussian curves was

$$f(x) = A\ e^{\frac{-4\log 2}{\Gamma^2}(x-x_o)^2},$$

where A is the maximum height of the peak and x_o is the value of x when $f(x) = A$, i.e. $f(x_o) = A$. Fig. 5 shows the two resulting Gaussian curves. The smaller curve is for $\theta = 90^\circ$ and the larger is for $\theta = 180^\circ$. The statistical error for the total number of counts in each photopeak is of the order of 0.6%, so the statistics here are quite reliable. The error in the areas taken can be safely attributed entirely to the uncertainty involved in moving a needle along a line by eye. This error is overwhelmingly greater than any error inherent in the planimeter itself. An estimate of this error was made by taking the area

---

[1] See page 40a.

1

The principal purpose for fitting Gaussian curves to the photopeaks was to strip away the contribution on the left due to the Compton distribution and the slight contribution on the right due to the small coincidence peak at 1.33 Mev. The Gaussian curves which were used each fitted their respective experimental coincidence peaks extremely closely (almost exactly) above the half-maximum height, and deviated appreciably from the experimental peaks only below the half-maxima, where the undesired contributions became appreciable. Initially, the peeling away had been done only by eye and the ratio of the number of counts in each peak was taken to get the asymmetry. The result using this method was $A = 1.145$. It was decided that a Gaussian, fitted to the experimental curve, would be a more accurate method of stripping away undesired contributions.

Fig. 5

Co^{60} Asymmetry

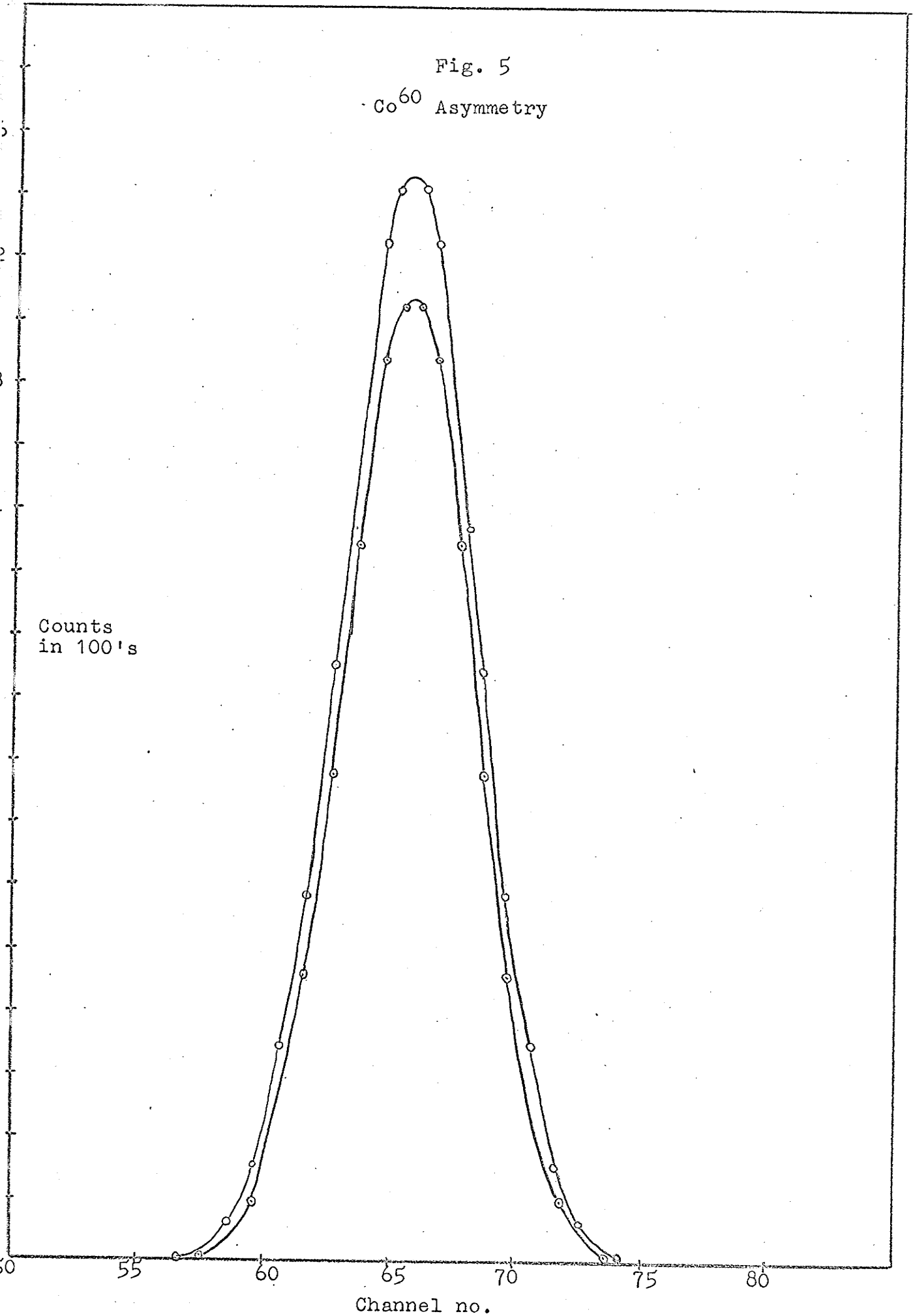

several times. The deviation from the mean indicated an error of no more than 0.5% in any given reading. This means that any given ratio has a possible error of about 1% attached to it.

The three ratios calculated yielded the results A = 1.152, 1.156, 1.160. The mean value is A = 1.156 with an average deviation from the mean of 0.003. To get an estimate of the error involved, a ratio was calculated by tracing out the outside edge of the two curves. This yielded an asymmetry $A_{outside} = 1.149$. Also, $A_{inside} = 1.168$. These two ratios suggest that an error of ±0.010 is reasonable, and in fact quite conservative. The result then is $A = 1.156 \pm 0.010$.

Na^{22} Isotropy

Na^{22} decays by positron emission mostly to the 1.28 Mev level of Ne^{22}. As the second test of the angular correlation spectrometer, the correlation function between the 1.28 Mev gamma and the 0.511 Mev annihilation gamma was measured. Since a positron at rest, annihilating with an electron, produces an isotropic distribution of annihilation quanta, the correlation should be isotropic.

Initial correlation runs indicated isotropy for spectrometer positions 1 to 9 (i.e. from $\theta = 90^{\circ}$ to about $\theta = 170^{\circ}$), but as θ increased from 170° to 180°, the coincidence counting rate increased significantly for a wide gate on the 1.28 Mev

peak, and decreased significantly for a very narrow gate on the 1.28 Mev peak. This effect was not understood at first and many possible explanations (such as magnetic field effects and P.M. fatigue) were presented, checked out, but were all found to be unsatisfactory. Subsequent considerations led to the following explanation, which is the presently accepted one. Consider two cases - a very narrow gate on 1.28 Mev, and a very wide gate on 1.28 Mev.

Narrow Gate: Assume a gate about 90 kev wide, centred on the 1.28 Mev peak. Considering only the range of angles $90^{\circ} \leqslant \theta \leqslant 180^{\circ}$, the conclusion is reached that there should be isotropy for the range $90^{\circ} \leqslant \theta < 180^{\circ}$, but near 180°, $W(\theta)$ should decrease. The reason for this is as follows below.

The coincidences sought will occur when a 1.28 Mev photon enters the narrow gate of the gating crystal (fixed side) and a 0.511 Mev annihilation photon enters the movable crystal, within the allotted resolving time (35 nanoseconds). When such a coincidence occurs near $\theta = 180^{\circ}$, then the 1.28 Mev photon is accompanied by another annihilation photon. i.e. Both the 1.28 Mev photon and a 0.511 Mev photon enter the gating (fixed) crystal. If both are captured in the crystal, then the resultant optical combination will be too large to enter the gate. Thus the gate will not be opened and the coincidence

not registered, even though it is a genuine coincidence. For $90^{\circ} \leq \theta < 180^{\circ}$, if a 1.28 Mev photon is in coincidence with a 0.511 Mev photon, then the other annihilation photon will not enter the gating crystal and there will thus be no optical summing. The gate will then be opened and the coincidence registered.

Wide Gate: Assume a gate about 800 kev wide, from about 1.20 Mev to 2.00 Mev. It is easily seen that such a gate will yield the same $W(\theta)$ for $\theta < 180^{\circ}$ as did the narrow gate. This follows because even though the gate will be opened many more times, due to optical summing, than it was opened for the narrow gate, these extra coincidences can be registered only for θ near 180°. Thus for a wide gate there is isotropy for $90^{\circ} \leq \theta < 180^{\circ}$ and an increase in $W(\theta)$ near $\theta = 180^{\circ}$.

It follows from the above explanation that the correlation function will form a symmetric peak centred at $\theta = 180^{\circ}$, for a wide window, and a symmetric dip centred at $\theta = 180^{\circ}$, for a narrow window. It also predicts that the height of the peak will begin to decrease as the upper level of the gate is decreased below 1.8 Mev, which is the sum of the 0.511 Mev and 1.28 Mev photons. These predictions were followed up experimentally and were substantiated in all cases.

In the light of this explanation, the initial isotropy (up to $\theta = 170^{\circ}$) was seen to be the result desired.

Another correlation run was made (to obtain better statistics), and again the result was isotropy for $90^{\circ} \leqslant \theta < 180^{\circ}$, as required by theory. The number of coincidence counts involved at each position was of the order of 3000, and the deviation from the mean for the four positions considered was no more than 35. This lies well within the statistical error of $\sqrt{3000}$.

Chapter 6.

SELENIUM 75 INVESTIGATIONS

6.1 General:

The decay of 120 day Se^{75} and the resulting gamma rays from As^{75} have been studied by many workers and most aspects of the decay scheme are well established. The present study was undertaken to clarify some of the remaining uncertainties and controversial features of the decay scheme.

Fig. 6 illustrates the level scheme of As^{75} due to the decay of Se^{75} to it. The levels and gamma rays shown, with the exception of the 429 kev and 628 kev gammas, are all given in the Nuclear Data Sheets, (N.D.S.). The 305 kev gamma ray is not shown because it did not concern the investigations. The spins and parities on the extreme right are also copied from the N.D.S.

Fig. 7 shows the normal (singles) spectrum from Se^{75} up to and including the 402 kev peak. The spectrum was taken with a 1½"x1" NaI(Tl) Harshaw "Integral Line" scintillation detector.[1] Various peaks are identified with energies in kev of the known gamma rays, all of which have been observed and recorded previously. The remainder of the spectrum,

---

1 The author is indebted to Dr. S. K. Sen for the use of this crystal.

Fig. 6

Level Scheme of As^{75} Due to Decay of Se^{75}

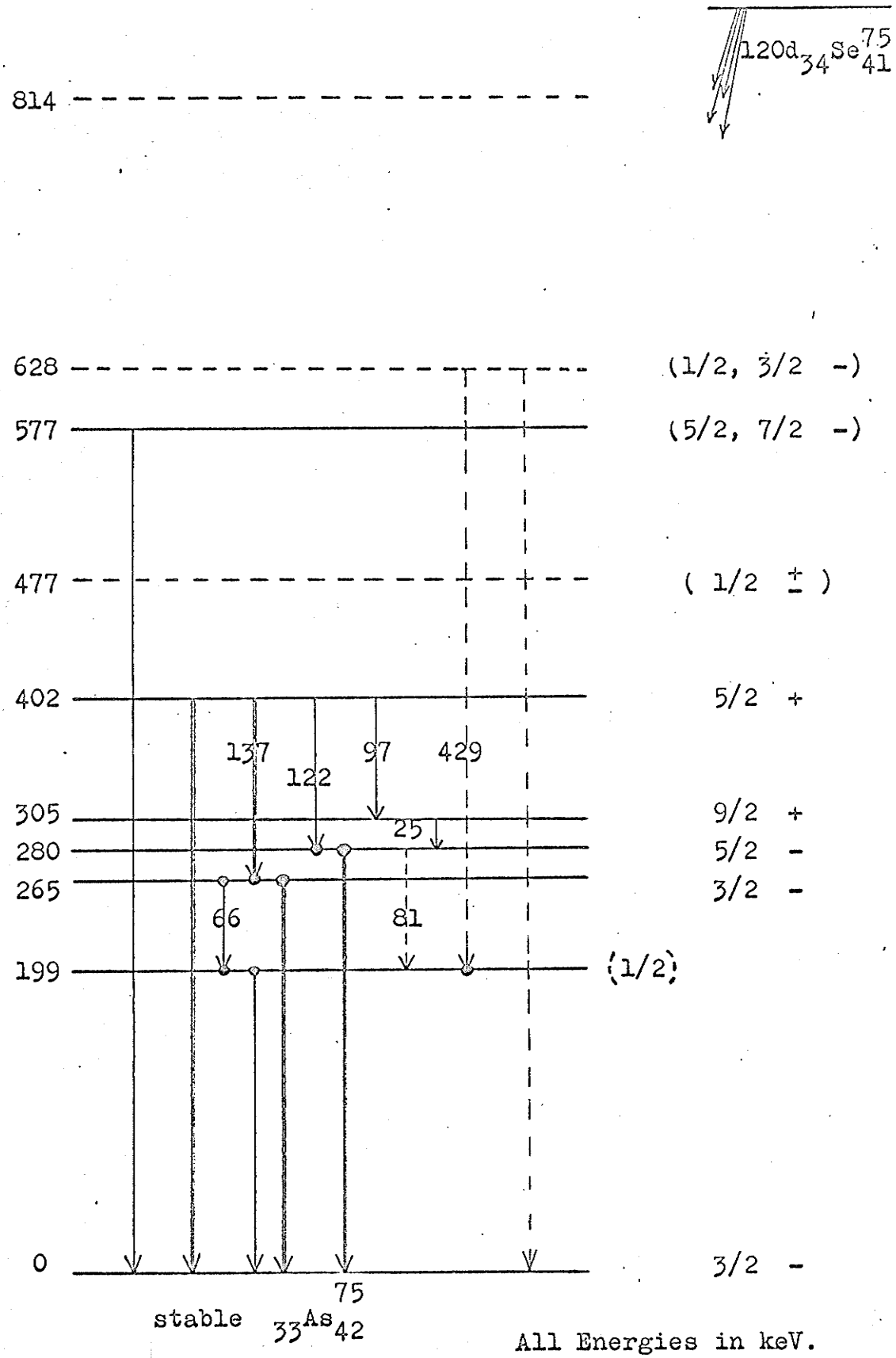

All Energies in keV.

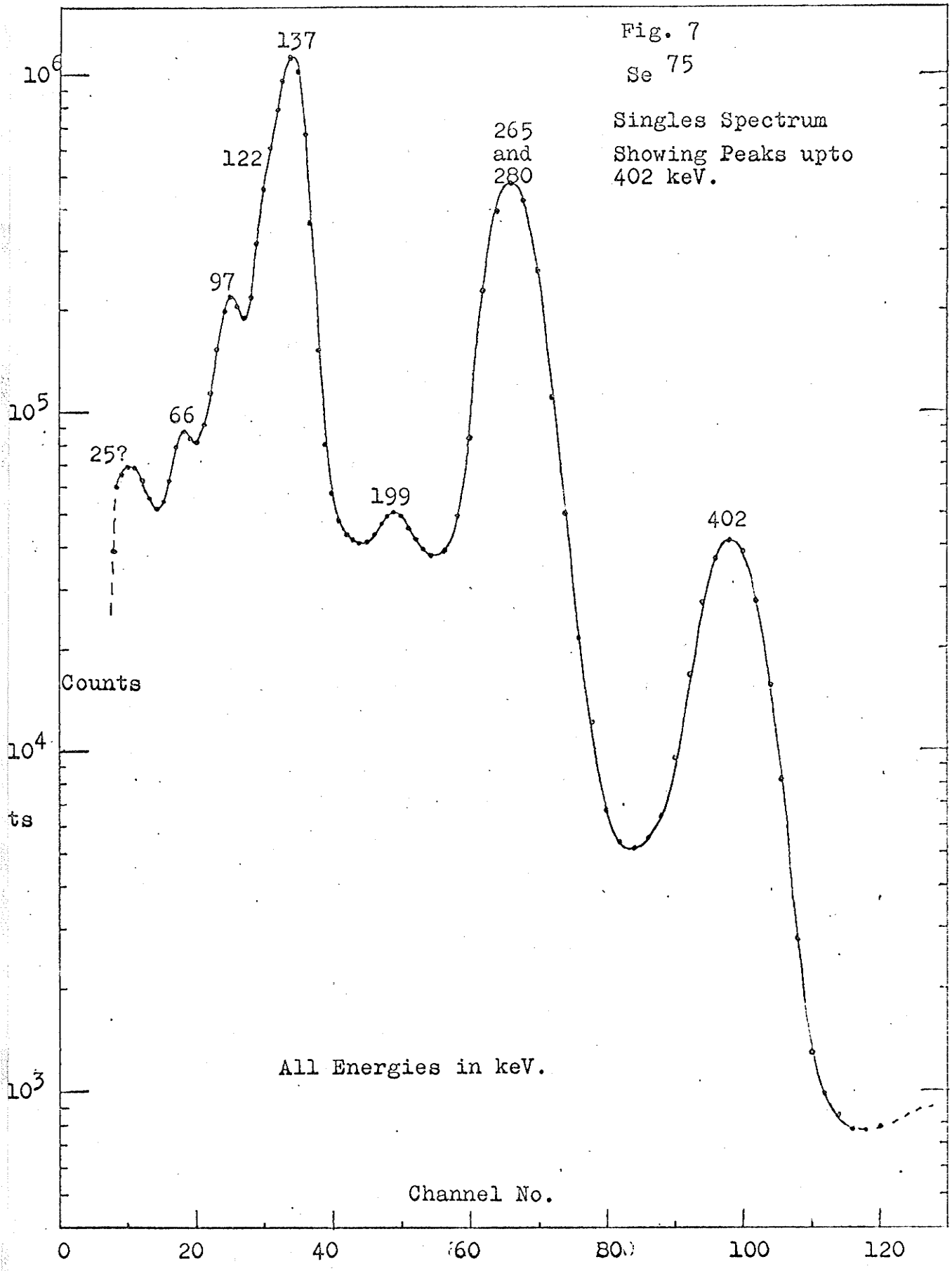
Fig. 7
Se 75
Singles Spectrum
Showing Peaks upto
402 keV.
137
122
265
and
280
97
66
25?
199
402
10^6
10^5
10^4
10^3
Counts
ts
All Energies in keV.
Channel No.
0
20
40
60
80
100
120

above 402 kev, was one of the subjects of the present study and will be presented later.

Some of the gamma rays in the energy region between 60 kev and 200 kev were investigated rather closely. Consequently an accurate calibration curve was required for this region in particular. The calibration sources found suitable for this purpose were:-

Ba^{131} --- 31.4 kev x-ray
Pb^{210} --- 47 kev gamma
Ba^{133} --- 81 kev gamma
Co^{57} --- 122 kev gamma
Se^{75} --- 199 kev gamma.

Fig. 8 shows the calibration curve for this energy region. Notice the non-linearity at low energies, mentioned earlier (chapter 2).

The decay scheme indicates several intense cascades. Examination of the branching ratios in the N.D.S. shows that, in particular, the 137-265, the 137-66-199, and the 122-280 cascades should produce relatively high coincidence counting rates. The author has, in fact, carried out coincidence runs for all of the above three cascades and has observed the high rates. However, the corresponding theoretical analyses have all been carried out by other workers and the results are well-established. Hence, no more need be said about these cascades.

Fig. 8

Low Energy Calibration Curve for NaI(Tl) Crystal

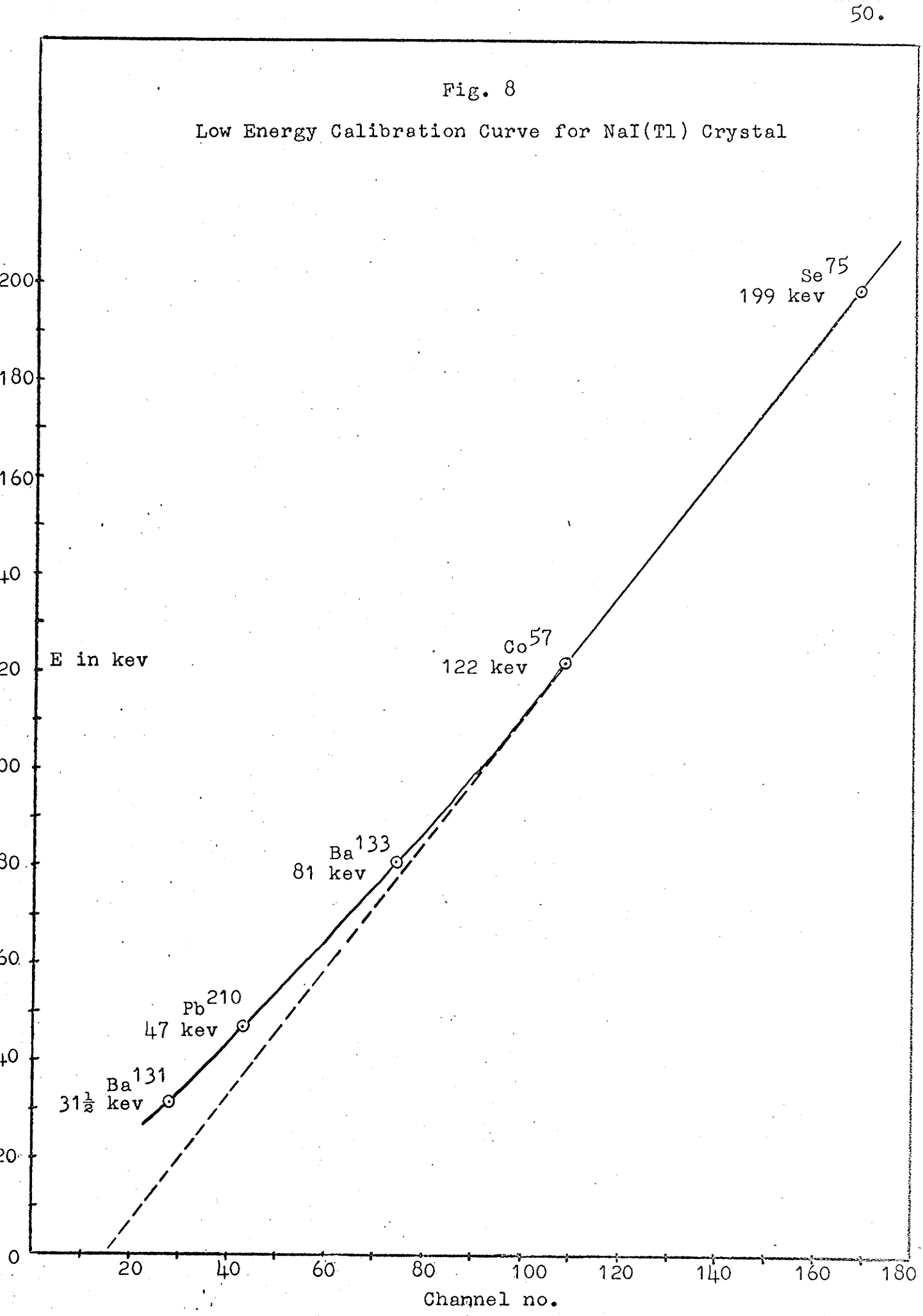

6.2 Gating on the 122 kev Peak:

The decay scheme indicates that the 122 kev gamma ray is in weak coincidence with an 81 kev gamma ray, as well as in strong coincidence with the 280 kev gamma ray mentioned in sec. 6.1. The 81 kev gamma ray, if it exists, must be of extremely weak intensity, as indicated by the very small branching ratio (1.3%)given in the N.D.S., and by the fact that the Se^{75} singles spectrum shows no trace of a peak due to an 81 kev gamma ray.

In the present study, a gate of about 10 kev (5 channels) was centred on the 122 kev, and a coincidence spectrum was obtained using two $1\frac{1}{2}$"x1" Harshaw "Integral Line" detectors[1] and a resolving time of 30 nanoseconds. The gate was set using a calibration curve because, as fig. 7 shows, the 122 kev peak lies on the left shoulder of the considerably more intense 137 kev peak. This latter fact meant that a large number of gating pulses would be of the 137 kev peak and thus the coincidence spectrum was essentially a superposition of the coincidence spectrum for a gate on 137 kev and that a gate on 122 kev. This being undesirable, the effect was partially avoided by gating only on the left side of the 122 kev peak, but to obtain a spectrum representative of only those pulses in coincidence with the 122 kev gamma ray, stronger means had to be employed. The method decided upon is described below.

---

1 The author is indebted to Dr. R. Connor for the use of one of these detectors.

The technique involves the obtaining of a coincidence spectrum using first a gate centred on the peak being considered, for some given time interval (10 hrs., say). Then the gate is moved to the left of the peak by an amount about equal to the gate width, and a 5 hour spectrum is subtracted from the original 10 hour spectrum. Finally, another 5 hour spectrum is subtracted using a gate displaced to the right of the peak by an amount equal to the left displacement. In all three cases, the gate widths, resolving times, and in fact all unit settings, are identical, with the exception of course, of the base line control, which determines the position of the gate.

The resulting coincidence spectrum, it is then hoped, shows all those gamma rays, and only those gamma rays, which are in coincidence with the gamma ray corresponding to the central gate. This technique is based upon the assumption that the undesired background appearing in the central gate has a certain shape, i.e., the assumption is that the central background is expressible as an average of the right and left backgrounds. Closer investigation indicates that this assumption is not an altogether unreasonable one. Notice also that if the gates are narrow, then the right and left hand gates will include pulses from the gamma ray being studied, as well as undesired background. However the former pulses will be far fewer in number than for the central gate, and in thus subtracting a few desired

counts, more confidence is gained that all those counts which remain unsubtracted are desirable.

The above described technique was carried out for the 122 kev peak. The resulting spectrum indicated that the 122 kev gamma is in coincidence with only the 280 kev peak. The rest of the spectrum was a series of small, irregularly shaped peaks and valleys, above and below the abscissa, except for a rather deep valley, about 650 counts below the abscissa, at 265 kev. This was due to the large negative count which had occurred for the right hand gate which was centred on the 137 kev peak, i.e., the 137-265 cascade is very intense.

This result suggests one of two things. Either there is no 81 kev gamma ray, or else the 137 kev gamma ray is in coincidence with a gamma ray in the vicinity of 81 kev to the degree of intensity that when the right hand gate is subtracted, the large negative coincidence count virtually "drags" down the peak of the weak intensity 81 kev gamma ray. In the next section this question will be resolved.

6.3 Gating on the 199 kev Peak:

Although the 199 kev peak is relatively isolated (and can thus be used as a calibration point), it is flanked on both sides by two peaks (the 137 kev and 265 kev peaks) which are far more intense than it is, and which also happen to be in

coincidence with each other. This unfortunate combination of circumstances produces a background in the 199 kev peak which will not only trigger the gate, but which will also provide an accompanying coincidence pulse. Such a situation appears to be "made to order" for the three gate subtraction technique described in sec. 6.2. When one of these background pulses opens the gate, one or more genuine but undesired coincidence pulses, in coincidence either with the 137 kev or 265 kev gamma rays, is allowed into the kicksorter. To get rid of these genuine but undesired coincidences, the three gate technique was used, with a gate about 20 kev wide (11 channels). Fig. 9 shows a singles spectrum of Se^{75} for energy up to and including the 265 kev and 280 kev peaks. A spectrum of the central gate is also shown superimposed on the former. The detectors were 1½"x1" Harshaw "Integral Line" detectors. The gating detector had a resolution of 7.5% at the 661 kev peak of Cs^{137} and the movable detector had a corresponding resolution of 8%. The accumulation times were 10 hours for the central gate (kicksorter in positive mode) and 5 hours each for right and left hand gates (kicksorter in negative mode).

Fig. 10 shows the resultant coincidence spectrum. A singles spectrum from the movable crystal (analysis side) has been superimposed on the coincidence spectrum and a calibration

Fig. 9

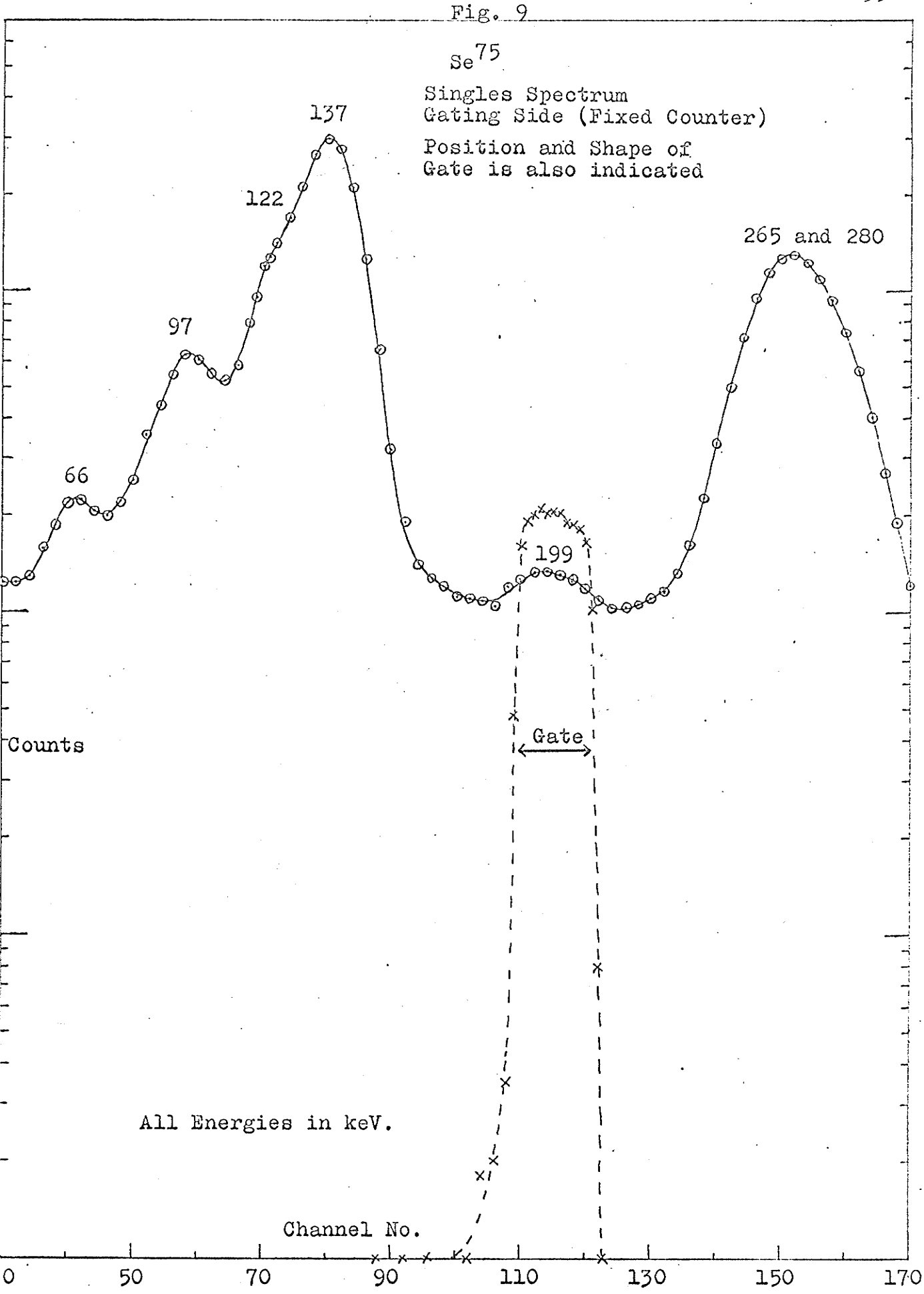
Se75
Singles Spectrum
Gating Side (Fixed Counter)
Position and Shape of
Gate is also indicated
137
122
97
66
265 and 280
199
Gate
Counts
All Energies in keV.
Channel No.
0
50
70
90
110
130
150
170

Fig. 10

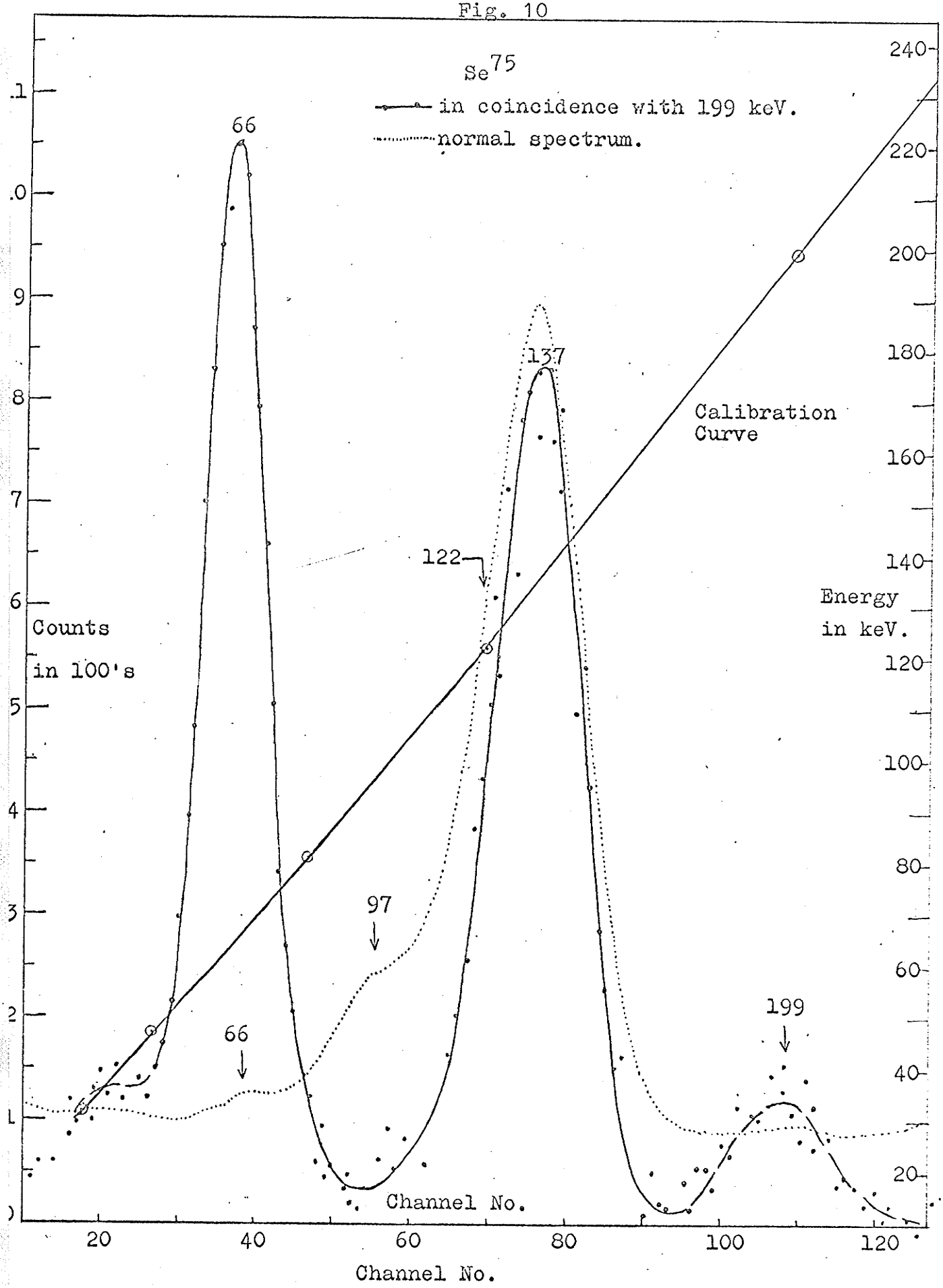
Se75
in coincidence with 199 keV.
normal spectrum.
66
137
122
97
66
199
Calibration Curve
Counts in 100's
Energy in keV.
Channel No.
Channel No.
240
220
200
180
160
140
120
100
80
60
40
20
.1
.0
9
8
7
6
5
4
3
2
1
0
20
40
60
80
100
120

curve has been included. Notice the striking appearance of the 66 kev peak in the coincidence spectrum. It rises even higher than the 137 kev peak, which is the highest peak in the singles spectrum. The reason no 81 kev peak was observed in sec. 6.2 is now clear. Even if there is an 81 kev peak, it would be "dragged" down to, or below the abscissa when a gate containing the 137 kev peak, to any appreciable extent, is subtracted.

Although the 81 kev gamma ray has never been observed in coincidence with another gamma ray, the decay scheme implies that it should also be in coincidence with the 199 kev gamma ray. The branching ratio given in the N.D.S. is 1.3%, a result reached using 180° spectrometer K-conversion electron considerations (32), (33).

Using the branching ratios given in the N.D.S., consider the following calculations. The absolute intensity of the 66 kev gamma ray, given per 100 disintegrations of Se^{75}, is

(14% x 3%) + (76% x 54% x 3%) 100 = 1.65/100 disintegrations.

Considering the coincidence spectrum of fig. 10 again, notice that there is only an extremely small hint, if any, of a peak at 81 kev. In fact, a very conservative estimate would make the intensity of the 81 kev peak certainly no more that 0.5% of

the intensity of the 66 kev peak. This would make the absolute intensity of the 81 kev gamma ray

$$0.5\% \times 1.65 \doteqdot 0.01 \text{ / } 100 \text{ disintegrations.}$$

According to the decay scheme, the absolute intensity of the 81 kev gamma ray, not taking into account the internal conversion, should be

$$(1.3\% \times 10\%) + (1.3\% \times 81\% \times 8\% \times 76\%) + (1.3\% \times 18\% \times 76\%)\ 100$$
$$= 0.37 \text{ / } 100 \text{ disintegrations.}$$

According to the K shell internal conversion coefficients tabulated on page 350 in Segre (22), the conversion coefficient for $k = 0.15$, $Z = 35$, and E2 radiation, is $\alpha_2 = 1.97$. The spin and parity of the 199 kev level are uncertain, and if perchance the parity is positive, then the radiation would be M2, and $\beta_2 = 2.74$. Thus we can expect the conversion coefficient to be about 2, at worst, for $Z = 33$. If this is taken into account, the intensity of the 81 kev gamma ray should be

$$\frac{0.37}{3} \doteqdot 0.1 \text{ / } 100 \text{ disintegrations}$$

as compared with an upper limit of

$$0.01 \text{ / } 100 \text{ disintegrations}$$

obtained from fig. 10.

Fig. 10 also shows a small, but unmistakable peak at about 200 kev. This suggests that there exists in the decay scheme a gamma ray of energy about 200 kev, heretofore unreported, in coincidence with the 199 kev gamma ray. According to the

decay scheme, this new gamma ray would necessarily come from a transition between the 402 kev and 199 kev levels. Several more coincidence spectra, like fig. 10, were obtained using different angles θ between the detectors. The coincidence peak at 200 kev was seen to decrease in size as θ was increased from $\theta = 90^{\circ}$ to $\theta = 180^{\circ}$. In fact, at $\theta = 180^{\circ}$, there was no peak at all at 200 kev. Furthermore, the position of the peak showed a slight but unmistakable angular dependence. This latter observation suggested a scattering effect wherein a gamma ray is Compton scattered in one counter and then reaches the second counter, thus registering a real coincidence. To determine if this were indeed merely a scattering effect, the detectors were set at 90° one from another, 0.5 in. of lead was placed between them, and another coincidence run was taken. As suspected, there was no peak whatsoever at 200 kev, thus ruling out the 402 $\longrightarrow$ 199 kev transition.

The gain of L.A. #1 (analysis side) was lowered such that the analysis side now gave a singles spectrum up to and including the 511 kev peak of Na^{22}, which peak was used as a calibration point. A coincidence run was then carried out, using again the three gate subtraction technique, to search for gamma rays above 137 kev, which may be in coincidence with the 199 kev gamma ray. In particular, Varma and Eswaran (34) have reported a 429 kev gamma from the transition 628 $\longrightarrow$ 199 kev,

in coincidence with the 199 kev gamma ray. The resultant spectrum from the 11 hour run (11 hours central gate and $5\frac{1}{2}$ hours right and left hand gates) had very good statistics (66 kev peak was 2600 counts high) but indicated virtually no peaks above the 137 kev peak. In particular, the number of counts in the channel corresponding to 429 kev was 6 counts, and since the number of counts in any given channel above 400 kev varied between only ± 15 counts, it can be said that there is no 429 kev gamma ray in coincidence with the 199 kev gamma ray. This contradicts the findings in reference (34). It should be noted also that the detector resolutions in the present investigation were considerably better than those of reference (34).

A directional correlation run was carried out using a gate on the 199 kev peak. The N.D.S. gives $(\frac{1}{2})^-$ as the spin and parity of the 199 kev level, derived only from log ft considerations. The brackets indicate a certain degree of uncertainty in this value.

Consider the cascade, $J_\alpha (L_\rho) J_\beta (L_\sigma) J_\gamma$, illustrated in sec. 3.2. Notice that if $J_\beta = \frac{1}{2}$, then n^{max} in the expression for $W(\theta)$ must be $(J_\beta - \frac{1}{2})$. i.e. $n^{max} = 0$ and the expression for $W(\theta)$ reduces to just one term, a constant. Thus we have the result that $J_\beta = \frac{1}{2}$ implies an isotropic correlation function, i.e. independent of θ. However, while an isotropic result is consis-

tent with $J_p = \frac{1}{2}$, it does not prove that $J_p = \frac{1}{2}$ because it may be possible to have a mixing ratio δ which will also give isotropy.

The correlation run involved four fairly evenly spaced positions of the movable spectrometer arm and was preceded by the Na^{22} isotropy check described in sec. 5.4. The three gate subtraction technique was carried out at each of the four positions (8 hours central gate and 4 hours right and left hand gates), and the total number of counts in the 66 kev peak was determined for all four positions. Starting at position 1, where $\theta = 90^o$, and through positions 4, 9, and finally 11, where $\theta = 180^o$, the number of counts were respectively 4500, 4521, 4488, and 4457. The statistical error involved in a peak of about 4500 counts is about 67 counts. Clearly then, the above result may be considered isotropic well within the bounds of statistical error, thus supporting the suggestion of spin $\frac{1}{2}$ for the 199 kev level.

6.4 High-Energy Region:

A short singles run (a few minutes) using a moderately strong Se^{75} source (20 microcuries) quickly shows that any gamma rays of Se^{75} above 402 kev are of extremely weak intensity. Thus to obtain any information about such gamma rays,

either a very long count, or else a much stronger source is necessary.

The detector used was a 1½"x1" Harshaw "Integral Line" detector of excellent resolution (slightly less than 7.5% at the Cs^{137} 661 kev peak) and stability (virtually no drift detected over a period of several weeks). The Se^{75} was from Oak Ridge, and a 20 microcurie source was prepared in the University of Manitoba's radiochemical laboratory. The detector was inserted in a 1" thick cylindrical lead shield which kept the background count quite low.

Using no lead absorber in front of the crystal, several long singles runs were made (about 12 hours each), the first one going up to only 600 kev, the second up to 700 kev, the third up to 800 kev, and so on up to 1500 kev. Background counts were subtracted for each spectrum. The results were indeed surprising. They showed small but definite peaks at 480, 511, 536, 660, 760, 890, 1280, and 1450 kev. Since none of these gamma rays are reported in the literature, source contamination was immediately suspected. Different Se^{75} sources were obtained from various professors at the university, and each source produced a different high-energy spectrum, of varying degrees of similarity to the one described above. The sources mentioned above were all from Oak Ridge except for one

from Amersham. It is unlikely that the sources contained all these impurities on arrival from Oak Ridge or Amersham. On the other hand, several of the above listed energies can be associated with gamma rays of sources being used by various research groups here at the university. The same hypodermic needle was very likely used to prepare several different sources, thus contaminating the Se^{75} to a degree so slight as to be noticed only for long singles counts. The 1450 kev was likely due to the K^{40} in the walls of the laboratory.

10 millicuries of Se^{75} was obtained from Chalk River[1] and without removing the bottle of Se^{75} from the can it arrived in (to prevent contamination from local sources), a 12 hour singles run was taken including energies up to 1500 kev. After background was subtracted the spectrum indicated only one definite peak above 402 kev, but its energy could not be accurately determined because of the accidental sum peaks of the far more intense 121, 137, 265, 280, and 402 kev gamma rays. Lead absorbers were used to filter out the lower energy gamma rays and it was found that 1.75 cm. of lead almost completely stopped the summing effect, any thicker absorber resulting merely in a reduced counting rate.

A 26 hour singles run was made including energies up to 900 kev, and using 1.75 cm. lead absorber. Background was subtracted and fig. 11 shows the result. The statistics

---

1 Atomic Energy of Canada Limited, Commercial Products, P.O. Box 93, Ottawa, Canada.

Fig. 11

Se^{75} Singles
(with 1.75 cm. lead absorber)

High Energy (> 402 kev) Spectrum

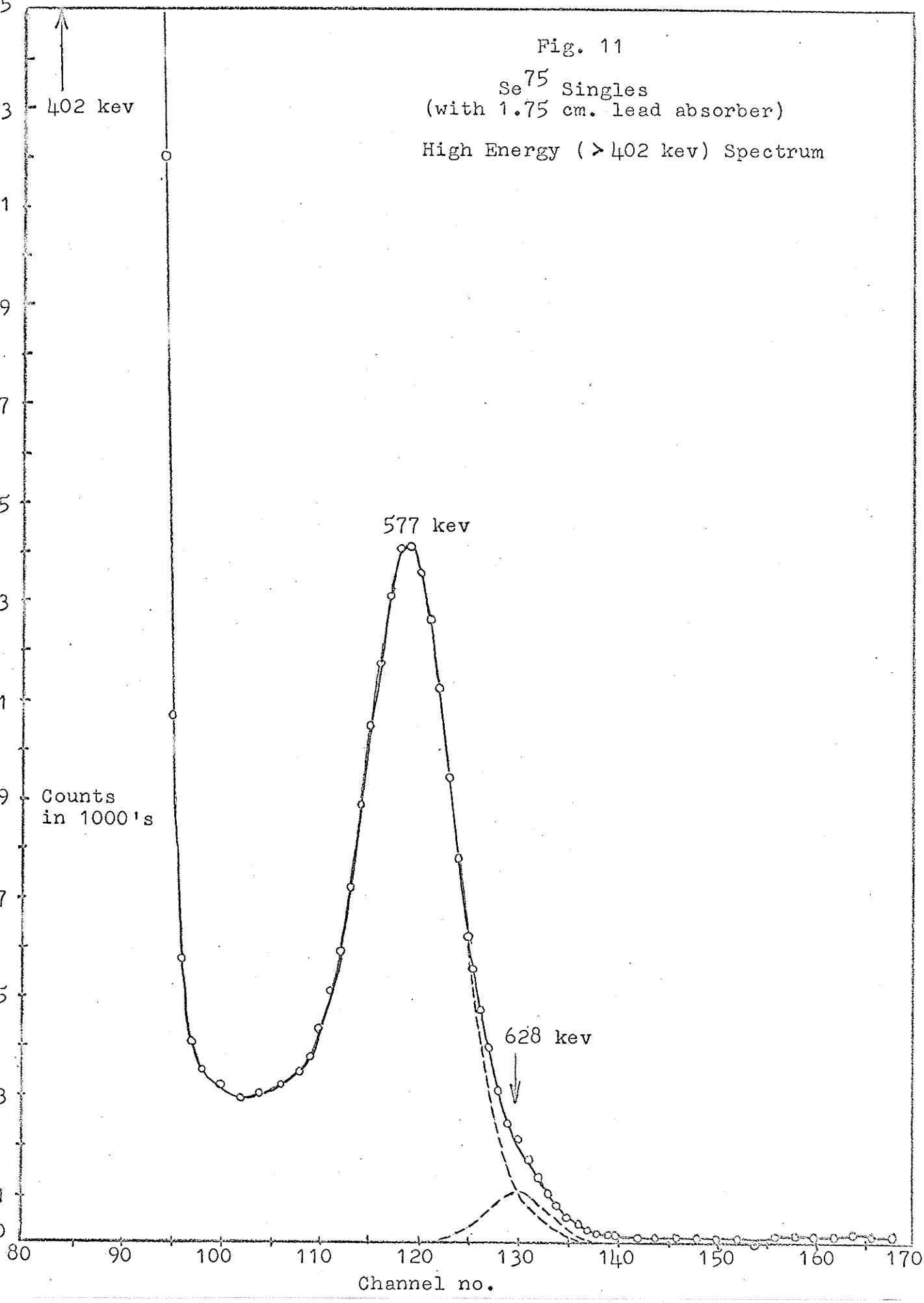

are excellent (the 577 kev peak is 14,000 counts high) and there is only a very slight hint (if any!) of a peak at 628 kev on the right shoulder of the 577 kev peak. Channel 83½ corresponds to 402 kev, channel 119 corresponds to 576 kev ± 3 kev, and channel 170 corresponds to 840 kev. As fig. 11 shows, there are no gamma rays above 628 kev and the ratio of the intensity of the 628 kev gamma ray to the intensity of the 577 kev gamma ray is found to be at most 0.03, an order of magnitude smaller than the ratio 0.2 obtained by Varma and Eswaran (34).

6.5 Conclusion (35):

The results are summarized on the decay scheme (fig. 6). The levels and gamma rays shown by solid lines along with the coincidences therein are all given in the N.D.S., and the present investigation has confirmed them. However, the levels and gamma rays shown by dotted lines and the coincidences therein have not been substantiated by the present investigation. In particular, Varma and Eswaran (Phys. Rev. 125, 656, 1962) have published a decay scheme which includes the 628 kev level with an associated 628 gamma ray and 429-199 cascade. The effect of the present investigation would be to remove all the "dotted" features of the decay scheme, as far as the decay of Se^{75} is concerned.

The spin value of $\frac{1}{2}$ for the 199 kev level, up to now derived only on the basis of log ft values in beta transitions, is also substantiated by the present investigation because the measured isotropic correlation in the 199-66 kev gamma-gamma angular correlation is consistent with this spin assignment.

It should be stressed that in searching for extremely weak intensity high energy gamma rays in a source with several, lower energy strong intensity gamma rays, great care must be taken to filter out the low energy gammas. Also, the source should be radiochemically pure to a high degree because even a very slight contamination can be very important when such low intensities are being considered. This in fact, may explain the peak observed at 628 kev by Varma and Eswaran.

The angular correlation spectrometer and associated electronics were found to be quite reliable after the inevitable "bugs" were removed. A pulse height spectrum stabilizer would, however, be most advisable, because in the present investigations, many hours were lost due to drifting of peaks. Furthermore, the automatic mode could not be utilized to anywhere near its full potential because of the manual drift corrections which had to be performed regularly (sometimes as often as every half hour, depending on the detectors used). Also,

the alignment and leveling accommodations are rather crude, and before an angular correlation run, one must spend a day or two merely leveling and aligning the detectors for all angles θ.

REFERENCES

(1) Roulston, K. I., Ph.D. Thesis, Univ. of Man. (1952).

(2) Naqvi, S. I. H., Ph.D. Thesis, Univ. of Man. (1961).

(3) Evans, R. D., "The Atomic Nucleus", McGraw-Hill Book Co., Inc., (1955).

(4) Siegbahn, K., "Beta and Gamma Ray Spectroscopy", North-Holland Publishing Co. (1955).

(5) Curran, S. C. and Baker, W. R., U.S. Atomic Energy Commission Report. MDDC. 1296, 17th Nov. (1944); Rev. Sci. Instr. 19, 116 (1948).

(6) Marshall, F. H. and Coltman, J. W., Phys. Rev. 72, 528 (1947).

(7) Marshall, F. H., Coltman, J. W. and Hunter, L. P., Rev. Sci. Instr. 18, 504 (1947).

(8) Marshall, F. H., Coltman, J. W. and Bennet, A. I., Rev. Sci. Instr. 19, 744 (1948).

(9) ~~Kallman, H., Natur und Technik, (July, 1947); Phys. Rev. 78, 621 (1950).~~ Birks, J.B., "Theory and Practice of Scintillation Counting", Macmillan, 1964.

(10) Bell, P. R., Phys. Rev. 73, 1405 (1948).

(11) Hofstadter, R., Phys. Rev. 74, 100 (1948).

(12) McIntyre, J. A. and Hofstadter, R., Phys. Rev. 78, 617 (1950).

(13) Pringle, R. W. and Standil, S., Phys. Rev. 80, 762 (1950).

(14) West, H. I., Meyerhof, W. E. and Hofstadter, R., Phys. Rev. 81, 141 (1951).

(15) Bannerman, R. C., Lewis, G. M., and Curran, S. C., Phil. Mag. 42, 1097 (1951).

(16) Eriksen, V. O. and Jenssen, G., Phys. Rev. 85, 150 (1952).

(17) Taylor et al, Phys. Rev. 84, 1034 (1951).

(18) Dhar, S., Indian J. Phys. 29, 329 (1955).

(19) Freedman et al, Phys. Rev. 89, 302 (1953).

(20) Bernstein, W., Nucleonics, 14, No. 4, 46 (1956).

(21) Engelkemeir, D., Rev. Sci. Instr. 27, 589 (1956).

(22) Segre, E., Experimental Nuclear Physics vol. III, Wiley (1959).

(23) Blatt, J. M. and Weisskopf, V. F., Theoretical Nuclear Physics, Wiley, (1952).

(24) Biedenharn, L. C. and Rose, M. E., Rev. Mod. Phys. 25, no. 3, 729 (1953).

(25) Siegbahn, K., "Alpha, Beta, and Gamma-Ray Spectroscopy", North-Holland Publishing Co. (1965).

(26) Feingold, A. M. and Frankel, S., Phys. Rev. 97, 1025 (1955)

(27) Manning, G. and Bartholomew, G. A., Phys. Rev. 115, 401 (1959).

(28) Gingell, C. E. L., IEEE Transactions on Nucl. Sc., pp. 32-43, (July, 1963).

(29) Chase, R. L., I.R.E. Transactions, NS-8, (July, 1961).

(30) Chase, R. L., Rev. Sci. Instr. 31 (1960).

(31) Emmer, T. L., I.R.E. Transactions, NS-9, (1962).

(32) Cork, J. M. et al, Phys. Rev. 79, 889 (1950).

(33) Schardt, A. W. and Welker, J. P., Phys. Rev. 99, 810 (1955).

(34) Varma, J. and Eswaran, M. A., Phys. Rev. 125, 656 (1962).

(35) Naqvi, S. I. H. and Dilay, A. J., Bull. Am. Phys. Soc., 10, 425, AB8 (1965)